END
DATE
FILMED
6-79
DDC

AFML-TR-78-121

LEVEL

HOT SALT STRESS CORROSION STUDIES

R. L. Fowler and A. J. Luzietti
Pratt & Whitney Aircraft Group
United Technologies
West Palm Beach, Florida 33402

1 JUNE 1978

Final Technical Report for Period 1 April 1976 - 1 June 1978
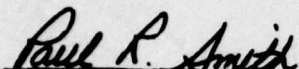
D D C
RECEIVED
MAY 8 1979
C

79 05 07 091

NOTICE

When Government drawings, specifications, or other data are used for any purpose other than in connection with a definitely related Government procurement operation, the United States Government thereby incurs no responsibility nor any obligation whatsoever; and the fact that the Government may have formulated, furnished, or in any way supplied the said drawings, specifications, or other data is not to be regarded by implication or otherwise as in any manner licensing the holder or any other person or corporation or conveying rights or permission to manufacture, use,or sell any patented invention that may in any way be related thereto.
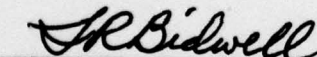
This report has been reviewed by the Information Services (NTIS). At NTIS, it will be available to the general public, including foreign nations.

This technical report has been reviewed and is approved for publication.

Paul R. Smith

PAUL R. SMITH
Program Manager

FOR THE COMMANDER

L.R. Bidwell

LAWRENCE R. BIDWELL
Actg. Chief,
Structural Materials Branch
Metals & Ceramics Division

If your address has changed, if you wish to be removed from our mailing list, or if the addressee is no longer employed by your organization, please notify AFML/LLS, WPAFB, Oh 45433 to help us maintain a current mailing list."

Copies of this report should not be returned unless return is required by security considerations, contractual obligations, or notice on a specific document.

REPORT DOCUMENTATION PAGE		READ INSTRUCTIONS BEFORE COMPLETING FORM
1. REPORT NUMBER AFML TR-78-121	2. GOVT ACCESSION NO.	3. RECIPIENT'S CATALOG NUMBER
4. TITLE (and Subtitle) HOT SALT STRESS CORROSION STUDIES.		5. TYPE OF REPORT & PERIOD COVERED Final Report. 1 April 1976 through 1 June 1978
		6. PERFORMING ORG. REPORT NUMBER PWA FR-10247
7. AUTHOR(s) R. L. Fowler A. J. Luzietti		8. CONTRACT OR GRANT NUMBER(s) F33615-76-C-5155
9. PERFORMING ORGANIZATION NAME AND ADDRESS United Technologies Corporation Pratt and Whitney Aircraft Group Government Products Division West Palm Beach, Florida 33402		10. PROGRAM ELEMENT, PROJECT, TASK AREA & WORK UNIT NUMBERS 61102 735302 02
11. CONTROLLING OFFICE NAME AND ADDRESS Air Force Materials Laboratory Air Force Systems Command Wright Patterson Air Force Base, Ohio 45433		12. REPORT DATE 1 June 1978
		13. NUMBER OF PAGES 55
14. MONITORING AGENCY NAME & ADDRESS(If different from Controlling Office) 58p.		15. SECURITY CLASS. (of this report) Unclassified
		15a. DECLASSIFICATION/DOWNGRADING SCHEDULE

16. DISTRIBUTION STATEMENT (of this Report)

Approved for public release, distribution unlimited

17. DISTRIBUTION STATEMENT (of the abstract entered in Block 20, if different from Report)

18. SUPPLEMENTARY NOTES

19. KEY WORDS (Continue on reverse side if necessary and identify by block number)

Hot Salt Stress Corrosion	Threshold Stress
Titanium	Low-Cycle Fatigue
Ti-6-2-4-2	Fatigue
Beta Processed	Microstructure
Alpha-Beta Processed	Simulated Flight-Cycle

20. ABSTRACT (Continue on reverse side if necessary and identify by block number)

Cyclic hot salt stress corrosion (HSSC) of Ti-6-2-4-2 bolthole specimens has been characterized under Air Force Materials Laboratory Contract F33615-76-C-5155. Effects of various flight-cycle simulations, maximum temperature, and microstructure were investigated using a concept analogous to a low-cycle fatigue (LCF) study. Isothermal stress cycling increased HSSC threshold stress over static loading. Simultaneous stress/temperature cycling increased threshold stress (and cyclic life) over isothermal stress cycling. A simple takeoff/shutdown dwell simulation produced the highest test results of the thermal-mechanical cycles investigated, with no significant effect from the addition of idle and cruise components. HSSC susceptibility increased with increasing maximum cyclic temperature. Alpha-beta processed material showed better resistance to HSSC than did beta material.

DD FORM 1473 1 JAN 73 EDITION OF 1 NOV 65 IS OBSOLETE

iii

TABLE OF CONTENTS

LIST OF ILLUSTRATIONS

LIST OF ILLUSTRATIONS (Continued)

LIST OF TABLES

viii

SECTION I

INTRODUCTION

The program consisted of a 26-month two-phase technical effort to define the HSSC behavior of Ti-6Al-2Sn-4Zr-2Mo (Ti 6-2-4-2) alloy under conditions of cyclic temperature and stress which are relevant to a gas turbine engine compressor disk service environment. The objective of the program was to develop a laboratory test which would confirm what had become apparent from engine experience, i.e., under current engine operating conditions HSSC does not develop although it could be predicted by current titanium HSSC curves based on static loading conditions. It is anticipated that these data will provide a stepping stone to the development of a prediction system for cyclic HSSC behavior in titanium high-pressure compressor and low-pressure turbine disk applications.

During Phase I, the effects of various simulated components of a disk flight-cycle (i.e., idle, takeoff, cruise, and shutdown) on cyclic HSSC behavior were investigated. Testing was confined to beta processed Ti-6-2-4-2 at a 950°F simulated takeoff temperature. Phase I test results provided the basis for selection of the cycle for Phase II testing, incorporating those portions of a disk flight-cycle which influence HSSC behavior.

Phase II testing was performed on both beta and alpha-beta materials to establish the effect of varying microstructure and takeoff temperature on cyclic HSSC behavior. Beta material was tested at 800 and 1100°F takeoff temperatures and alpha-beta material was investigated at 800 and 950°F.

Due to the large number of mission-cycles investigated, it was impossible to statistically substantiate each S-N curve within the time and total number of specimens defined for this contract. However, enough data points were generated to draw firm conclusions concerning the effects on HSSC behavior of the various parameters investigated.

1

SECTION II

BACKGROUND

Both alloy developments and process developments on alloys such as Ti-8Al-1V-1Mo and Ti-6Al-2Sn-4Zr-2Mo have been successful in continually upgrading the creep capability of these materials over the past decade. New engine models have taken full advantage of the higher creep strength improvements by utilizing titanium materials to replace nickel-base superalloys in the high-pressure compressor. The results have significantly impacted engine technology by reducing compressor rotor weights and allowing a cost effective replacement of nickel-base superalloy materials. Advanced engine designs may soon, for the first time, incorporate an all titanium compressor rotor, and applications in the low-pressure turbine stages may be within reach. Numerous investigators (Reference 1) have demonstrated that, under certain conditions of temperature, stress, and exposure to halide salts, titanium alloys are susceptible to embrittlement and premature cracking. This phenomenon has been called hot salt stress corrosion (HSSC) and is of particular interest to the gas turbine engine designer because the conditions required to cause HSSC seem to be fulfilled by titanium compressor components of current engines (References 2 and 3).

Although there have been instances of HSSC in titanium during alloy processing developments and during engine test stand operation (Reference 4), there have been no documented component service failures attributable to this phenomenon.

Other investigations into the nature of HSSC of titanium alloys have usually involved elevated temperature monotonic loading of a salt exposed rupture type specimen at various stress levels for approximately 100 hr. Test temperatures have varied from 500 to 1000°F. After the static loading period, the specimens were examined for stress corrosion cracking and usually subjected to an ambient temperature tensile test to determine residual ductility. Thus, each set of test conditions was judged either to cause or not to cause HSSC or embrittlement. For a given temperature, the stress below which HSSC did not occur was established and was designated the HSSC threshold stress. Thus, curves for 100-hr exposure threshold stress have been established for most titanium compressor component alloys.

H. R. Gray (Reference 5) has demonstrated that exposure with simultaneous cycling of both temperature and stress results in reduced susceptibility to HSSC compared to that caused by isothermal, monotonic loading exposure. Thus, it can be inferred that flight variables could act synergistically to prevent or ameliorate HSSC cracking. This conclusion was confirmed at P&WA Commercial Products Division (Reference 6) where testing incorporating a simulated compressor disk notch feature, a bolthole specimen, was accomplished under static loading conditions, cyclic temperature/constant stress, isothermal/cyclic stress, and simultaneous cyclic temperature and stress.

Based on these background data, this test program was initiated to study HSSC under conditions more closely simulating actual flight engine loading cycles. It was anticipated that the results would provide insight into reasons for the discrepancy between laboratory predictions of HSSC occurrence and actual engine experience.

SECTION III

MATERIALS

Four Ti-6-2-4-2 disk forgings (F100 turbine plates, P/N 1SZ 4042715) were procured to supply material for beta processed Phases I and II test specimens. The disks (Figure 1) were isothermally beta forged from 9-in. diameter multiples at Tβ + 50°F in the Ladish Co. vacuum GATORIZING® rig on existing molybdenum tooling. In the isothermal process, the die sets and the forging multiple are preheated to the desired forging temperature and forged in a single operation. After forging, the disks are solution treated at 1790°F (1 hr) AC and aged at 1100°F (8 hr) AC.

A half forging, P/N 2F 744107, heat code LZUN-2003, was obtained from a production run of JT9D forging for Phase II specimens. This disk/hub was all alpha-beta processed and solution treated and aged at Tβ − 25°F (1 hr) AC + 1100°F (8 hr) AC in accordance with the PWA 1209 specification.

BETA PROCESSED TI-6-2-4-2

Mechanical property evaluation of the subject beta processed disks included room temperature (RT) and 900°F tensile tests, room temperature notched time to fracture (RTNTF) tests, and creep tests at 1050°F/25 ksi.

Test specimens were machined from the integral test ring location of each disk and tested by the forging vendor while additional specimens were machined from the outer periphery (rim) of each of the disks and tested at P&WA. While a formal P&WA specification for all beta processed Ti-6-2-4-2 has not been established, the following tentative levels are being considered:

RT Tensile:	130 ksi UTS, 120 ksi YS, 8% El, 15% RA
900°F Tensile:	90 ksi UTS, 70 ksi YS, 10% El, 20% RA
RTNTF:	170 ksi/5 hr/No failure
Creep:	35 hr minimum to 0.1%, plastic deformation at 1050°F/25 ksi.

These properties were used as criteria to which the subject disks were compared.

The RT tensile properties of the beta processed material generally exceeded the minimum proposed requirements of beta processed Ti-6-2-4-2 presented above. Ultimate tensile strength for all specimens ranged from 140 to 145 ksi while 0.2% yield strengths were 120.5 to 128 ksi. The percent elongation and reduction of area ranges were from 8.5 to 14% and 12.2 to 23.0%, respectively. Two values below the 15% minimum reduction of area were recorded. At 900°F, all proposed specification properties were met with the exception of two integral test ring specimens which were about 1 ksi below the yield strength requirement. The 900°F ultimate tensile strength, 0.2% yield strength, percent elongation, and percent reduction of area values were 91.1 to 101.4 ksi, 69.2 to 77.1 ksi, 13.0 to 16.7%, and 27.4 to 45%, respectively. All data are shown in Table 1.

Notched rupture specimens (K$_t$ = 3.8) from the beta material were loaded at 170 ksi and run for 5 hr minimum. No failures occurred. Integral test ring specimens were discontinued at this point; however, specimens machined from rim locations were uploaded 10 ksi every 5 hr to failure. Rupture loads were 190 to 200 ksi for the specimens from each of the disks. All data are shown on Table 2.

Figure 1. Isothermally Beta Forged Ti-6Al-2Sn-4Zr-2Mo Disk Type Forgings for HSSC Test Specimens

4

TABLE 1. TENSILE PROPERTIES OF ISOTHERMALLY BETA FORGED AND SOLUTION TREATED AND AGED Ti-6Al-2Sn-4Zr-2Mo ALLOY DISK FORGINGS[1]

Disk S-N	Specimen No.	Specimen Location	Temperature (°F)	0.2% YS (ksi)	UTS (ksi)	El (%)	RA (%)
1	112-1	Int Test Ring	RT	124.9	144.0	14.0	22.0
	1-20	Rim Tangential	RT	120.5	141.4	12.2	16.3
2	112-2	Int Test Ring	RT	122.9	140.3	10.0	23.0
	2-16	Rim Tangential	RT	124.5	141.2	8.5	22.4
3	112-3	Int Test Ring	RT	127.5	145.4	9.0	22.0
	3-16	Rim Tangential	RT	126.6	144.7	10.4	13.5
4	112-4	Int Test Ring	RT	124.4	142.4	9.0	20.0
	4-20	Rim Tangential	RT	127.7	145.1	11.8	12.2
1	212-1	Int Test Ring	900	69.2	93.0	16.0	41.0
	1-19	Rim Tangential	900	76.0	97.7	16.0	38.9
2	212-2	Int Test Ring	900	70.1	91.1	13.0	41.0
	2-15	Rim Tangential	900	76.2	100.0	14.9	35.6
3	212-3	Int Test Ring	900	71.8	94.2	15.0	45.0
	3-15	Rim Tangential	900	77.1	101.4	13.7	27.4
4	212-4	Int Test Ring	900	69.8	93.4	15.0	42.0
	4-19	Rim Tangential	900	73.5	96.7	16.7	31.4

[1]Heat Treatment = 1790°F (1) AC + 1100°F (8) AC.

TABLE 2. ROOM TEMPERATURE NOTCHED STRESS RUPTURE (K_t=3.8) PROPERTIES OF ISOTHERMALLY BETA FORGED AND SOLUTION TREATED AND AGED Ti-6Al-2Sn-4Zr-2Mo ALLOY DISK FORGINGS[1]

Disk S-N	Specimen No.	Specimen Location	Initial Stress	Final Stress	Time (hr)	Remarks
1	512-1	Int Test Ring	170	170	5	Discontinued
	1-21	Rim Tangential	170	190[2]	10.2	Ruptured
2	512-2	Int Test Ring	170	170	5	Discontinued
	2-17	Rim Tangential	170	200[2]	15.2	Ruptured
3	512-3	Int Test Ring	170	170	5	Discontinued
	3-17	Rim Tangential	170	200[2]	15.4	Ruptured
4	512-4	Int Test Ring	170	170	5	Discontinued
	4-21	Rim Tangential	170	190[2]	10.7	Ruptured

[1]Heat Treatment = 1790°F (1) AC + 1100°F (8) AC.
[2]Increased 10 ksi every 5 hr.

All beta processed specimens except one from the rim location of disk S/N 1 met the creep requirement of 35 hr to 0.1% plastic deformation at 1050°F/25 ksi. The specimen in question exhibited a 0.1% life of 25 hr. An additional specimen from this disk was retested at 1050°F/25 ksi and exhibited a 0.1% life of 57.9 hr. Creep lives of the remaining specimens ranged from 35 to 88 hr to 0.1% elongation. Results of creep testing are presented in Table 3.

5

TABLE 3. CREEP PROPERTIES OF ISOTHERMAL-LY BETA FORGED AND SOLUTION TREATED AND AGED Ti-6Al-2Sn-4Zr-2Mo ALLOY DISK FORGINGS[1]

Disk S-N	Specimen No.	Test Condition		Creep Time (hr)	
		Temperature (°F)	Stress (ksi)	0.1%	0.2%
1	712-1	1050	25	60	96
	1-17	1050	25	[2]25	110
2	712-2	1050	25	62	132
	2-13	1050	25	54	130
3	712-3	1050	25	88	154
	3-13	1050	25	42	91
4	712-4	1050	25	61	126
	4-17	1050	25	35	95

[1]Heat Treatment = 1790°F (1) AC + 1100°F (8) AC.
[2]Retest gave 57.9 hr to 0.1%.

Metallographic examination of selected specimens from the four beta processed disks revealed a microstructure of acicular alpha platelets arrayed in colonies with some outlining of prior beta grain boundaries by alpha (Figure 2). The microstructures are typical of those of beta processed Ti-6-2-4-2 alloy in the solution treated and aged condition.

ALPHA-BETA PROCESSED MATERIAL (PWA 1209)

Mechanical property evaluation by the material vendor of the subject alpha-beta processed disk included RT and 900°F tensile tests, RTNTF tests, and creep tests at 950°F/35 ksi. PWA 1209 specification mechanical properties requirements are listed below:

RT Tensile: 130 ksi UTS, 120 ksi YS, 10% El, 20% RA
900°F Tensile: 90 ksi UTS, 70 ksi YS, 15% El, 30% RA
RTNTF: 170 ksi/5 hr/No failure
Creep: 35 hr minimum to 0.1% plastic deformation at 950°F/35 ksi.

All tensile properties at both RT and 900°F met or exceeded the PWA 1209 specification requirements. The RT ultimate tensile and 0.2% yield strength ranges were 146 to 152 ksi and 134 to 139 ksi, respectively. The RT percent elongation and reduction of area ranges were 12 to 16% and 29 to 37%, respectively. Values for the 900°F ultimate tensile strength, 0.2% yield strength, percent elongation, and percent reduction of area were 99 to 105 ksi, 76 to 81 ksi, 18%, and 43 to 48%, respectively. All data are shown in Table 4.

Three notched rupture specimens ($K_t = 3.8$) were loaded at 170 ksi and run for 5 hr without failure. The RTNTF data are recorded in Table 5.

Two creep specimens were loaded to 35 ksi at 950°F. Both specimens met the PWA 1209 specification since plastic deformation had not reached 0.1% after 35 hr of testing in each case. Creep data are recorded in Table 6.

Metallographic examination of the alpha-beta processed forging revealed equiaxed alpha in a transformed beta matrix (Figure 3). The microstructure is typical of alpha-beta processed Ti-6-2-4-2 alloy in the solution treated and aged condition.

6
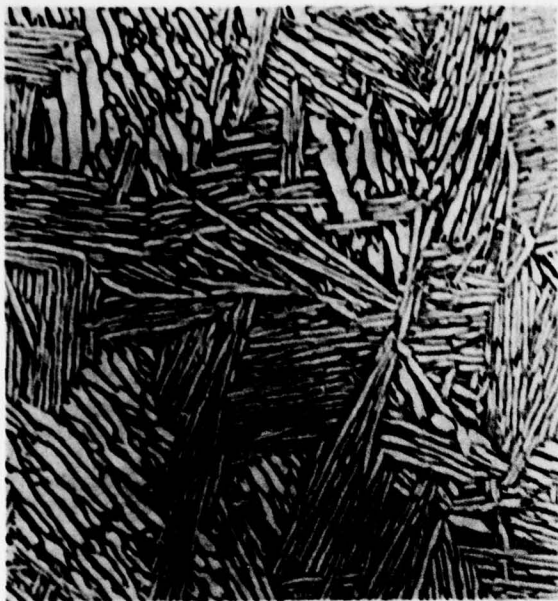
S/N 1
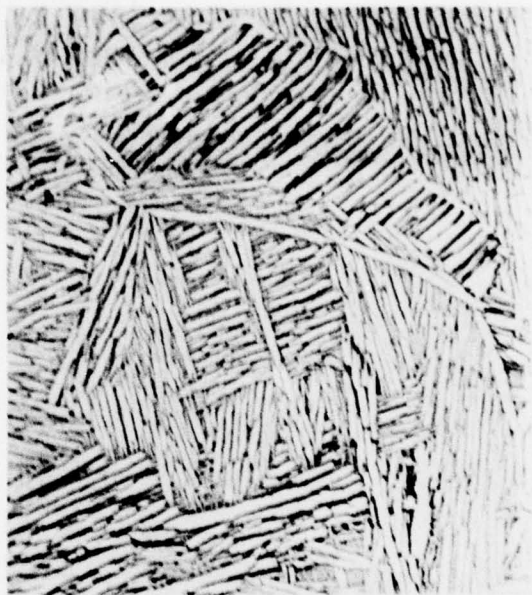
S/N 2

Mag: 250X   S/N 3

S/N 4

FD 143081

Figure 2.   Typical Microstructures of Isothermally Beta Forged Ti-6Al-2Sn-4Zr-2Mo

7

TABLE 4. TENSILE PROPERTIES OF ALPHA-BETA PROCESSED Ti-6Al-2Sn-4Zr-2Mo ALLOY (PWA 1209) JT9D 7th-STAGE COMPRESSOR DISK FORGING P/N 2F-744107

Heat Code: LZUN, Forging Serial No. 2003

Specimen No.	Temperature (°F)	0.2% YS (ksi)	UTS (ksi)	El (%)	RA (%)
1	RT	139.8	152.4	12	32
3	RT	137.7	150.1	14	36
6	RT	135.9	147.4	16	29
5	RT	136.7	151.5	14	34
8	RT	133.5	146.7	14	35
4	RT	134.5	147.2	16	37
PWA 1209 Requirement	RT	120.0	130.0	10	20
1	900	81.1	105.2	18	46
3	900	77.0	99.8	18	47
6	900	80.0	102.6	18	43
5	900	76.4	101.4	18	43
8	900	77.8	100.8	18	44
4	900	78.0	101.2	18	48
PWA 1209 Requirement	900	70.0	90.0	15	30

TABLE 5. ROOM TEMPERATURE NOTCHED STRESS RUPTURE ($K_t = 3.8$) PROPERTIES OF ALPHA-BETA PROCESSED Ti-6Al-2Sn-4Zr-2Mo ALLOY (PWA 1209) JT9D 7th-STAGE COMPRESSOR DISK FORGING

P/N: 2F-744107   Heat Code: LZUN   Forging Serial No. 2003

Specimen No.	Stress (ksi)	Time (hr)	Remarks
1	170	5.0	Did not fail
2	170	5.0	Did not fail
3	170	5.0	Did not fail
PWA 1209 Requirement	170	>5.0	Rupture *not* to occur in less than 5 hr at 170 ksi

TABLE 6. CREEP PROPERTIES OF ALPHA-BETA PROCESSED Ti-6Al-2Sn-4Zr-2Mo ALLOY (PWA 1209) JT9D 7th-STAGE COMPRESSOR DISK FORGING P/N 2F-744107

Heat Code: LZUN   Forging Serial No. 2003

Specimen No.	Temperature (°F)	Stress (ksi)	Time (hr)	El (%)	Remarks
1	950	35	20	0.08	
			36	0.10	
2	950	35	20	0.06	
			75	0.10	
			84	0.10	
PWA 1209 Requirement	950	35	35	0.10	Time to 0.1% creep to be not less than 35 hr

8
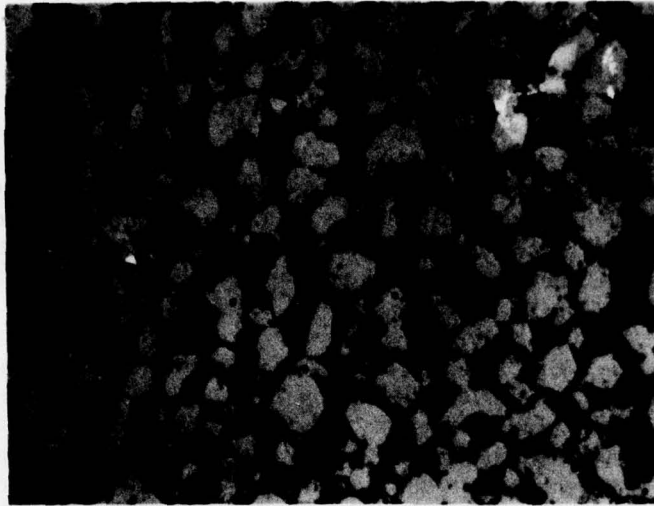
Mag: 500X

Figure 3.   Typical Microstructure of Alpha-Beta Processed Ti-6-2-4-2 P/N 2F-744107, LZUN-2003

SECTION IV

SPECIMENS AND SPECIMEN PREPARATION

Previous experience showed that areas of stress concentrations such as notches and boltholes are the most susceptible to HSSC. The specimen chosen for this study is shown in Figure 4. This specimen, designed to simulate a typical disk bolthole, has an elastic stress concentration factor (K_t) of 2.5. Specimens were machined to varying test section thickness to facilitate the attainment of different stress levels on a single series-loaded multiple-specimen test assembly.

The term "stress" as used throughout this report refers to the nominal net section stress, which is defined as the applied axial force divided by the minimum cross-sectional area through the bolthole. Calculation of the applicable area excludes the area occupied by the bolthole. For local stress determinations inside the bolthole, the elastic K_t is only applicable when this local stress is all elastic. It is recognized that, due to localized inelastic straining, the actual stress at a crack origin inside the bolthole is less than the nominal stress multiplied by the elastic K_t, but greater than the applied nominal stress. However, because of the complex cycle configurations and varying specimen thicknesses, it was not possible within the limited scope of this contract to determine the true stress/applied load relationships for all conditions.

Bolthole specimens for Phases I and II were machined from four beta processed forgings. Phase II alpha-beta specimens were machined from a JT9D 7th-stage compressor disk forging. After machining, the specimens were dimensionally and visually inspected and the center hole was chamfered by a butterfly polishing technique. Following this process the specimens were subjected to glass bead peening at an intensity of 10 to 12N. Peening was conducted at an automated facility at Metal Improvement Inc., Windsor, Connecticut. After peening, the specimens were washed in a solution of detergent and warm water, rinsed in hot deionized water, and allowed to air dry. All subsequent handling of the specimens was performed with surgical or cotton gloves to prevent salt contamination from handling.

After cleaning, the specimens were instrumented with thermocouples prior to salt application. Two thermocouples were tack welded opposite each other inside the bolthole on the load axis centerline of the specimen. Mechanical stress at this location is minimum in the bolthole (axial stress = zero) and thermocouple tack welds do not influence failure.

Salt was applied to test specimens by a technique developed at P&WA/Florida, by the chemistry section of the Materials and Mechanics Technology laboratories. In this technique a known quantity of simulated sea-salt solution per ASTM D-1141-62 was applied to a known area inside and around the bolthole. The saltwater was calibrated in terms of weight of chloride ions per metered drop. The appropriate quantity of saltwater was applied by metering a predetermined number of drops onto a preselected area which included the bolthole bore. A saturated wooden applicator was used to uniformly spread the measured sea-salt solution drops onto the area to be covered. Preheating the specimen permitted rapid water evaporation from the salt solution. To determine salted area, measurements of salted surfaces (except bolthole bore) were made from 1X photographs rather than from the specimen to minimize surface contamination. To ensure the proper salt concentration, a trial specimen which was salted at the same time as the test specimens was washed with deionized water which subsequently was analyzed for chloride ions by specific ion electrode.

10

2.880
2.870

2.880
2.870

5.760 Ref

1.102
1.098

2.204 Ref

0.437 to 0.439 Dia [A]
Do Not Break Sharp
Edges This Hole Only

[B]

0.750 to 0.751 Dia
Ream or Bore Smooth
(2 Places)

Gage Section

Gage Length

1.015
1.000

1.015
1.000

0.820
0.800

(2 Places)

32 GAA

As Specified

0.505 Ref
(2 Places)

0.500 - 0.550 R
Blend Smoothly
(4 Places)

Dimensions in Inches
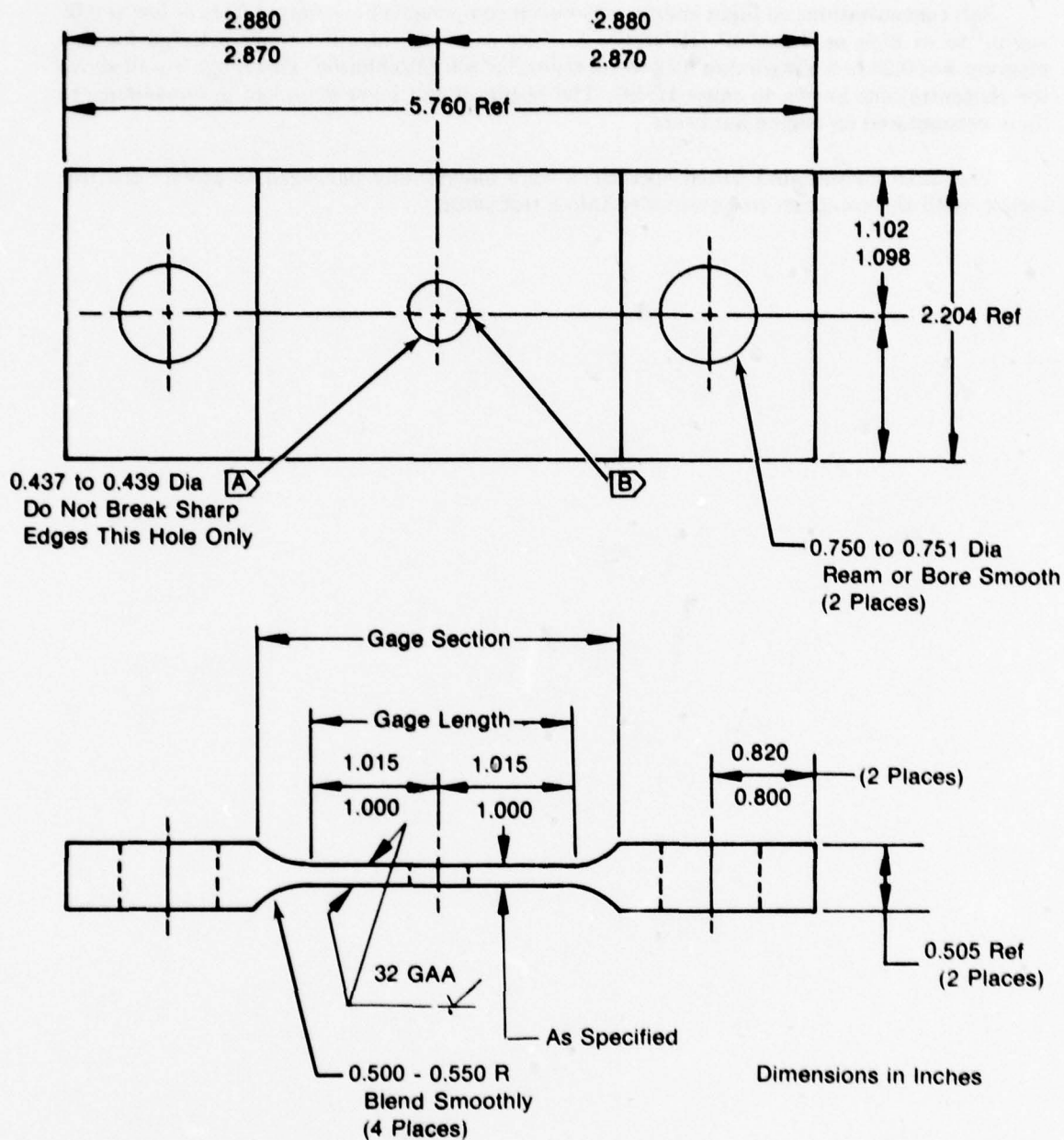
- Surface Finish Per Spec PWA 351
- Holes Must be on ₵ Within 0.002 FIR and Perp With Plane of Gage Section Within 0.002 FIR
- Gage Length Thickness Must be 0.180 - 0.210 for Drill and Bore of Hole [A]
- Gage Section Must be Ground
- Drill Hole [A] 27/64 Dia Thru Bore 0.437 to 0.439 Dia One Pass 600 ± 50 rpm
  Feed 0.002 In/Rev Cutting Fluid PMC 9252 "Broach Oil" Boring Tool Quill No. 267912-T-47
  Bit No. 254610-T-2-CN6F
- Any Unavoidable Withdraw Marks Must be at Location [B]

FD 143083

Figure 4. Bolthole Low-Cycle Fatigue Specimen

11

Salt concentrations on flight engine compressor components have ranged from as low as 0.05 mg/in.^{2} to as high as 5 mg/in.^{2} (Reference 3). The salt concentration range selected for this program was 0.25 to 2.5 mg/in.^{2},or 0.12 to 1.2 mg/in.^{2} of soluble chloride. This range is well above the concentrations known to cause HSSC. The resultant salt layer is typical in appearance to those encountered on engine hardware.

The instrumented and salted specimens were individually packaged to protect the test section until the specimen was assembled into a test setup.

SECTION V

EXPERIMENTAL PROCEDURE

Testing accomplished in this program incorporated thermal-mechanical simulated mission cycles in which both temperature and stress were cycled simultaneously to characterize Ti-6-2-4-2 HSSC behavior.

The test procedure for this program was altered from what has come to be the conventional method of characterizing HSSC behavior. In the conventional method, a series of specimens, loaded to different stresses are exposed for a predetermined period of time in an attempt to bracket the threshold stress. After exposure, all specimens are subjected to a room temperature loading, usually tensile loading increased to rupture, to determine which stresses produce HSSC or embrittlement. The threshold stress is established as the minimum stress required to produce HSSC. Of course there must be at least one (or more) stress corroded specimens and at least one (or more) unaffected specimens to establish the threshold bracket. Should the stress range selected produce HSSC in all specimens or produce no HSSC, the threshold stress cannot be established.

The testing outlined in this contract lent itself well to development of S-N curves (stress vs cycles to failure) used to express fatigue behavior. In the development of S-N curves, stresses are selected to produce failures over the cyclic life range of interest. Specimens are inspected periodically to establish the life to the first detectable crack, and from these data, crack initiation S-N curves are plotted. It is felt that this approach offers the following advantages over the conventional crack/no crack threshold stress method.

- Estimates of HSSC threshold stresses are possible for a wide range of exposure time using the same number of specimens which would be required to establish the threshold stress for one exposure time by the conventional techniques. Estimates of crack initiation lives over a range of stresses are also possible using the same data base.

- Crack initiation life curves do not require both stress corroded and unaffected tests to draw meaningful conclusions.

- Crack initiation curves provide a more useful tool for the design engineer to predict component service life.

- Cyclic HSSC behavior can be expressed in terms of cumulative number of cycles (analogous with number of flight missions) as well as in conventional terms of threshold stress for exposure time.

- Crack initiation curves can be compared with future unsalted baseline low-cycle fatigue data to establish stress corrosion degradation and to establish the groundwork for development of LCF/HSSC interaction relationships.

In Phase I of the program, beta processed material was subjected to eight different complex mission cycles all with a maximum (simulated takeoff) temperature of 950°F. The object of Phase I testing was to identify those components of the flight cycle (i.e., idle, takeoff, climb/cruise, and shutdown) which influence HSSC of Ti-6-2-4-2. Phase II evaluated the effect of varying microstructure (beta vs alpha-beta) and takeoff temperature on HSSC crack initiation.

All specimens were tested to failure except in a few cases where life extended beyond that anticipated. Some specimens were discontinued in order to accomplish all testing within the

13

schedule of the contract. Due to the large number of cycles evaluated and the limited number of data points per curve, it was not possible to generate statistically substantiated life curves. However, rudimentary S-N curves were developed which are adequate to demonstrate the effect of each simulated flight cycle on HSSC crack initiation.

PHASE I

Testing in Phase I was confined to the beta processed material. The eight simulated flight cycles used are illustrated in Figures 5 through 9. Each temperature/stress profile (see Section IV for discussion of specimen stress) indicates the variation of those parameters with time for each cycle.

Basic Cycle (Takeoff/Shutdown)

The Basic Cycle consisted of 5 min at takeoff temperature and stress followed by 5 min at shutdown (ambient temperature/no load) as shown in Figure 5. All other cycles were modifications of this cycle.

Cycle II (Cyclic Takeoff Stress/Constant Takeoff Temperature)

Cycle II was a 950°F isothermal cycle consisting of 5 min at takeoff stress and 15 min shutdown (Figure 6).

Cycle III (Takeoff/Shutdown) Resalting Effect

The Cycle III temperature/stress profile is the same as the Basic Cycle (Figure 5). A periodic resalting was incorporated for comparison with the single salt application of the Basic Cycle to determine the effect of salt application frequency.

Cycle IIIb (Extended Takeoff/Shutdown)

Cycle IIIb, shown in Figure 5, was similar to the Basic Cycle, but with the takeoff duration increased from 5 min to 15 min to evaluate the effect of a prolonged takeoff condition.

Cycle V (Idle/Takeoff/Shutdown)

Cycle V consisted of the addition of a 10-min, 300°F, low stress idle dwell to the Basic Cycle (Figure 7). The idle stress was established as 37.5% of the takeoff stress for each cycle.

Cycle VI (Idle/Takeoff/Cruise/Shutdown)

Cycle VI (Figure 8) consisted of the addition of a 30-min, 850°F, cruise dwell to the Cycle V configuration following the 5-min takeoff dwell. The cruise stress was established as 91% of the takeoff stress.

Cycle VII (Idle/Takeoff/Reduced Cruise/Shutdown)

Cycle VII was similar to Cycle VI with the 30-min cruise reduced to 15 min (Figure 8).

Cycle VIII (Takeoff/Hot Shutdown)

Cycle VIII, shown in Figure 9, was similar to the Basic Cycle, the ambient temperature/no load shutdown dwell being replaced by a 15-min, 200°F, low stress shutdown dwell. The Cycle VIII shutdown stress was established as 37.5% of the takeoff stress. The 200°F shutdown dwell was incorporated to simulate a short stop between flights when the heat soak-back on shutoff maintains some intermediate temperature until the next takeoff.
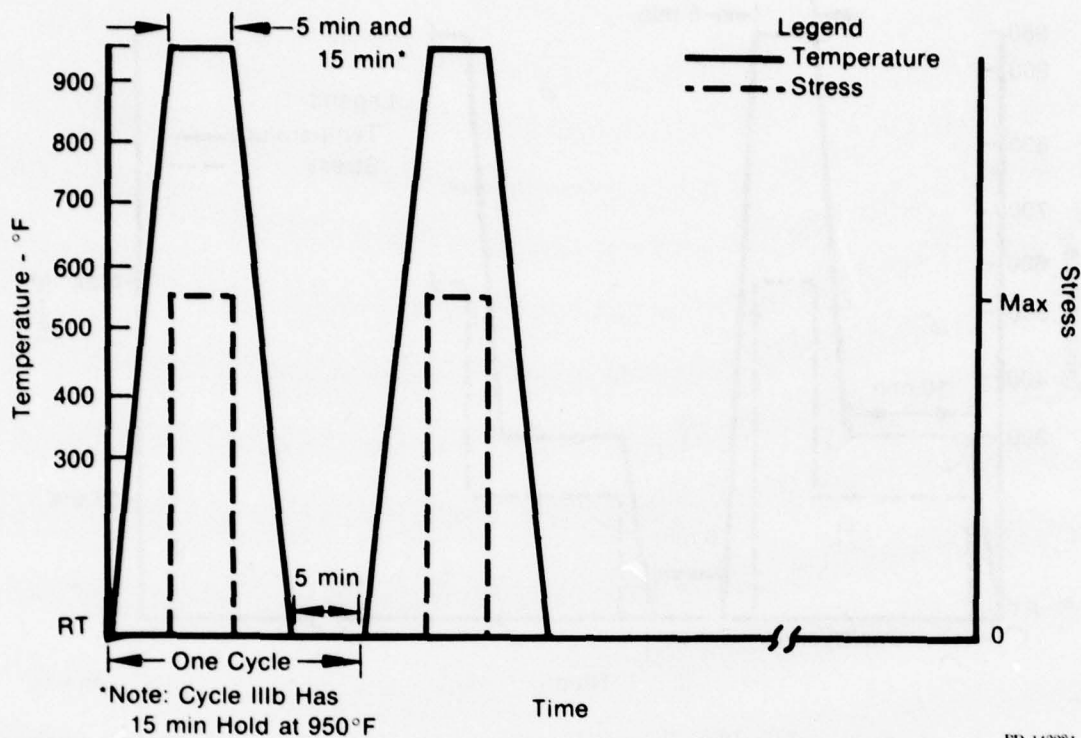
Figure 5. Basic Cycle, Cycle III (Resalt), and Cycle IIIb — Takeoff Plus Shutdown Dwell
Stress-Temperature Cycle Simulation
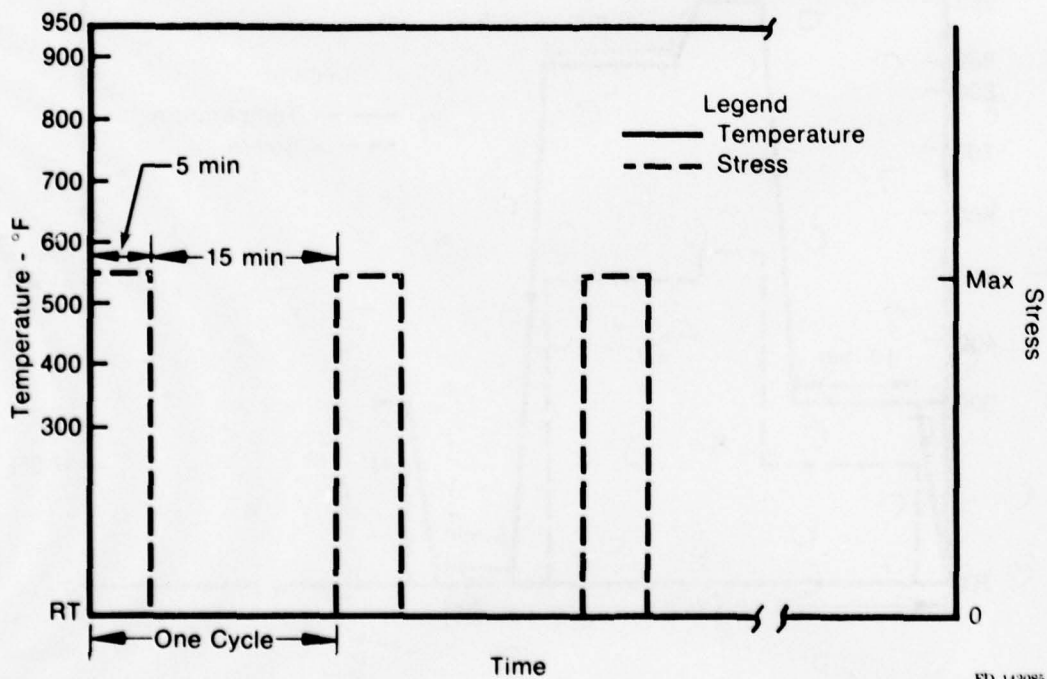
Figure 6. Cycle II —Takeoff Cyclic Stress-Constant Temperature Test

15
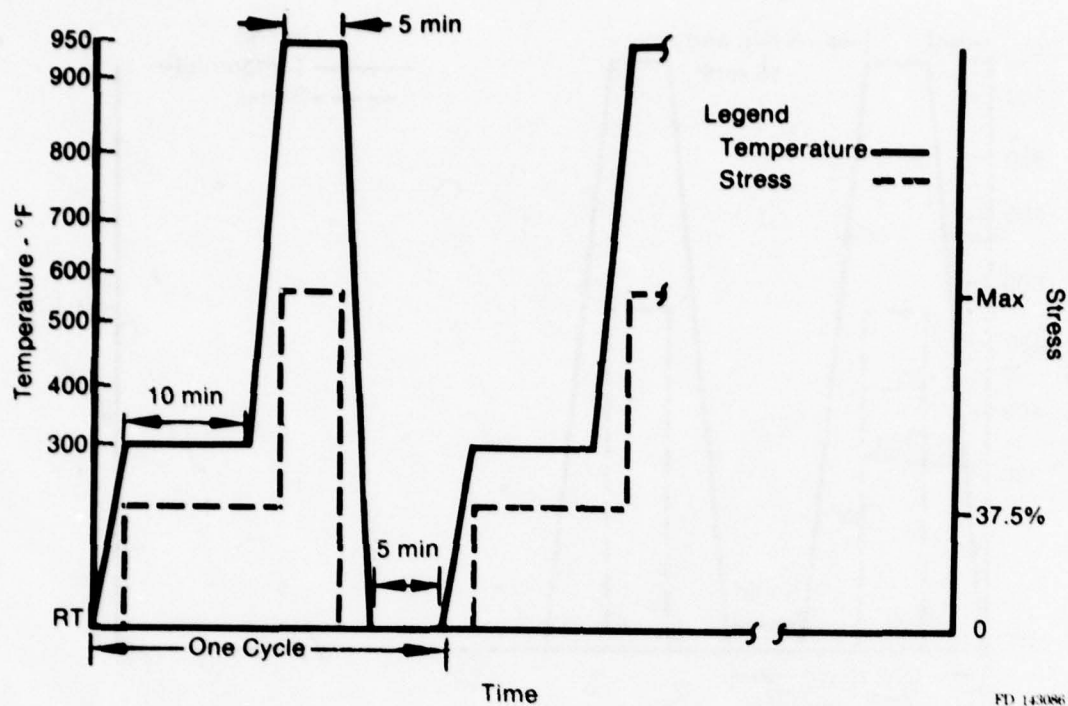
Figure 7. Cycle V — Idle Plus Takeoff Plus Shutdown Dwell Stress-Temperature Cycle Simulation
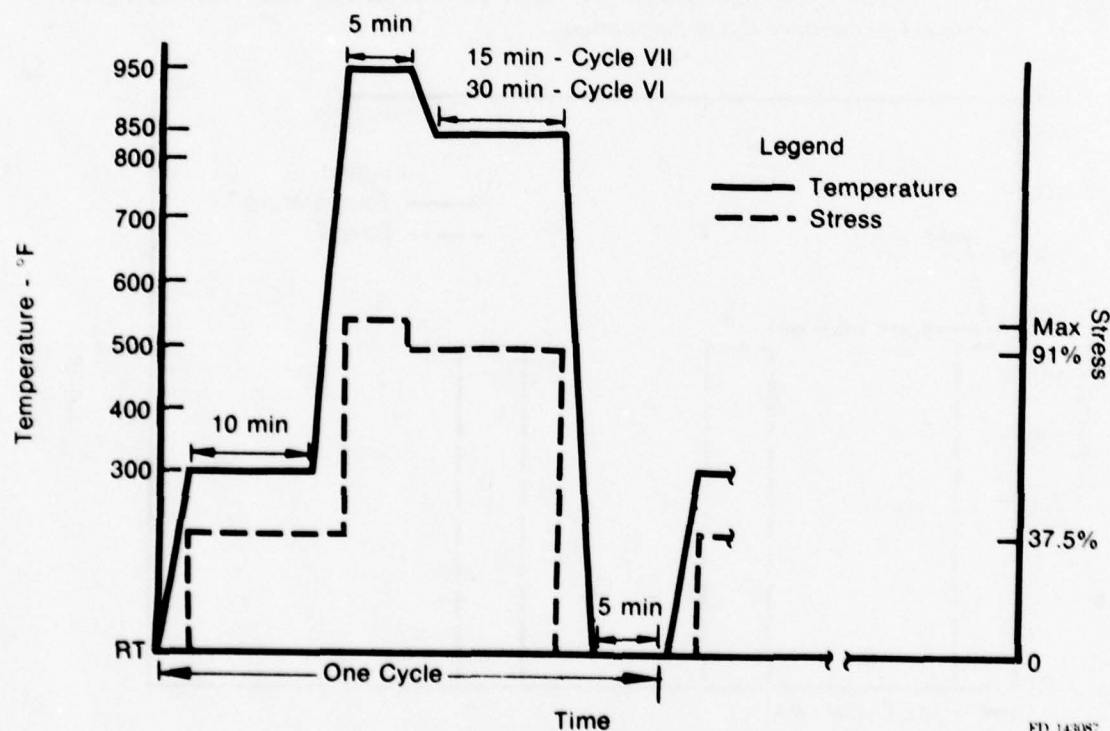
Figure 8. Cycles VI and VII — Idle Plus Takeoff Plus Cruise Plus Shutdown Dwell Stress-Temperature Cycle Simulation

16
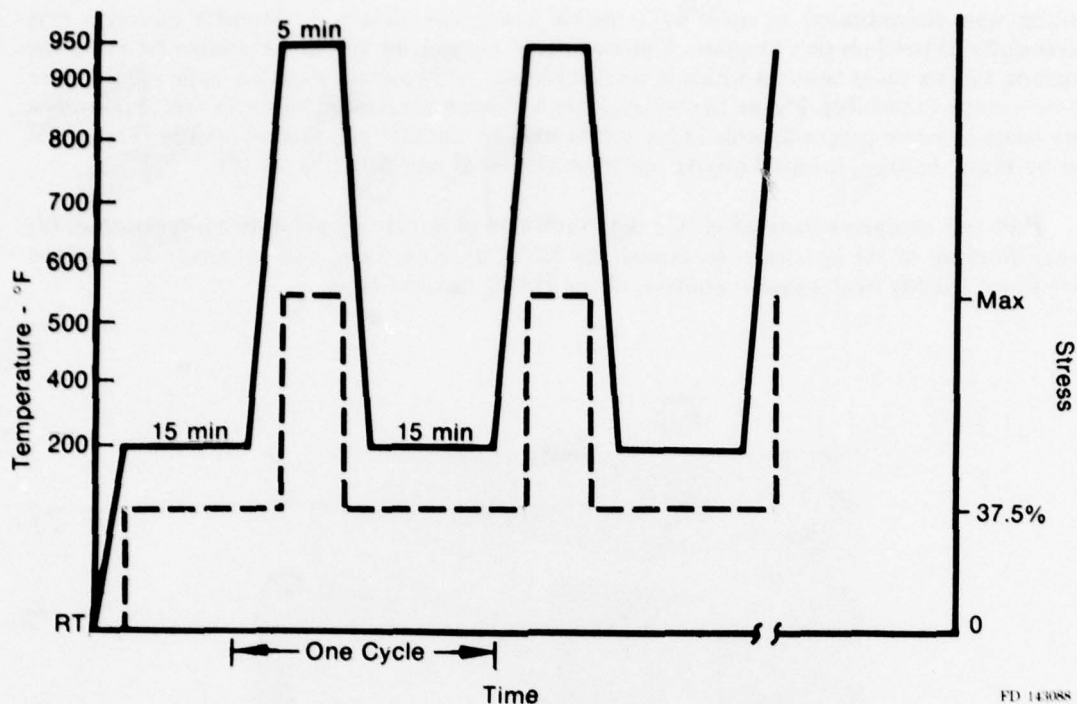
Figure 9. Cycle VIII — Takeoff Plus Hot Shutdown Dwell Stress-Temperature Cycle Simulation

PHASE II

Phase II testing was carried out on both beta and alpha-beta materials at various simulated takeoff temperatures to assess the effects of microstructure and temperature on cyclic HSSC behavior. From the results of Phase I testing Cycle VII (Figure 8) was selected as the test cycle for all Phase II testing.

Beta processed material was tested at 800 and 1100°F simulated takeoff temperatures for comparison with the 950°F Cycle VII tests of that material during Phase I.

Alpha-beta processed material was tested at 800 and 950°F takeoff temperatures for comparison with beta material tested at those temperatures.

Thermal-Mechanical Testing

Testing under this program was accomplished on three programmable servohydraulic, closed loop, thermal-mechanical LCF machines as shown in Figures 10, 11, and 12. Two specimens were series loaded in each machine. Specimens were machined to four different gage thicknesses so that stress differences of up to 15 ksi between two specimens could be achieved with a common load. All specimens were periodically inspected visually using a telemicroscope.

17

Testing was discontinued as soon as a visible crack was detected. Acoustic emission was successfully utilized on this program. Unfortunately, equipment was not available for all of the program, but on those tests on which it was employed, it frequently signaled impending failure before a crack was visible. Figure 13 shows the acoustic emission history of such a test. Specimens were heated by two programmable induction heaters on the first and second facility (Figure 14) and by radiation from infrared quartz lamps on the third machine (Figure 15).

Post-test analysis consisted of: (1) determination of remaining chloride concentration, (2) tensile fracture of the specimen to expose the HSSC fracture face, and (3) scanning electron microscope (SEM) fractographic analysis of the HSSC fracture face.

FC 39384A
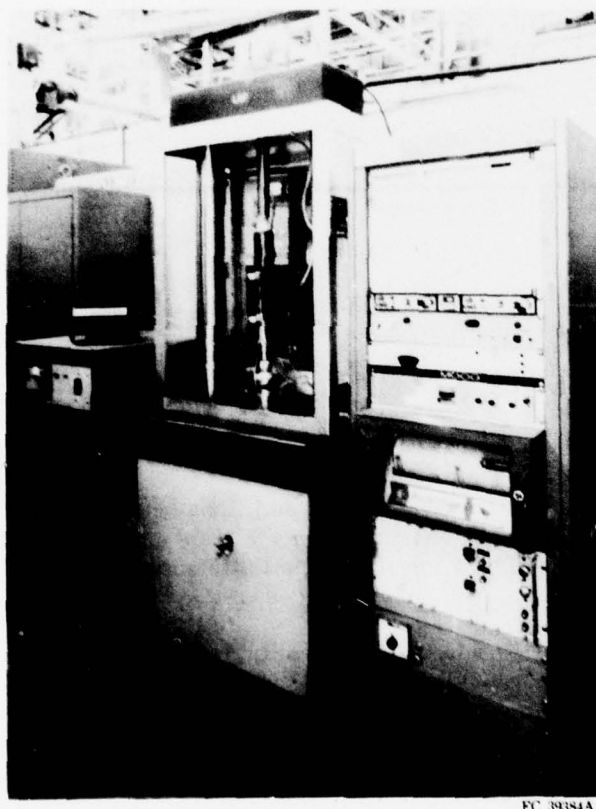
Figure 10. Thermal-Mechanical Low-Cycle Fatigue Rig No. LCF 3

18

FC 39382A

Figure 12. Thermal-Mechanical Low-Cycle Fatigue Rig No. LCF 2

FC 39390A

Figure 11. Thermal-Mechanical Low-Cycle Fatigue Rig No. LCF 5

19
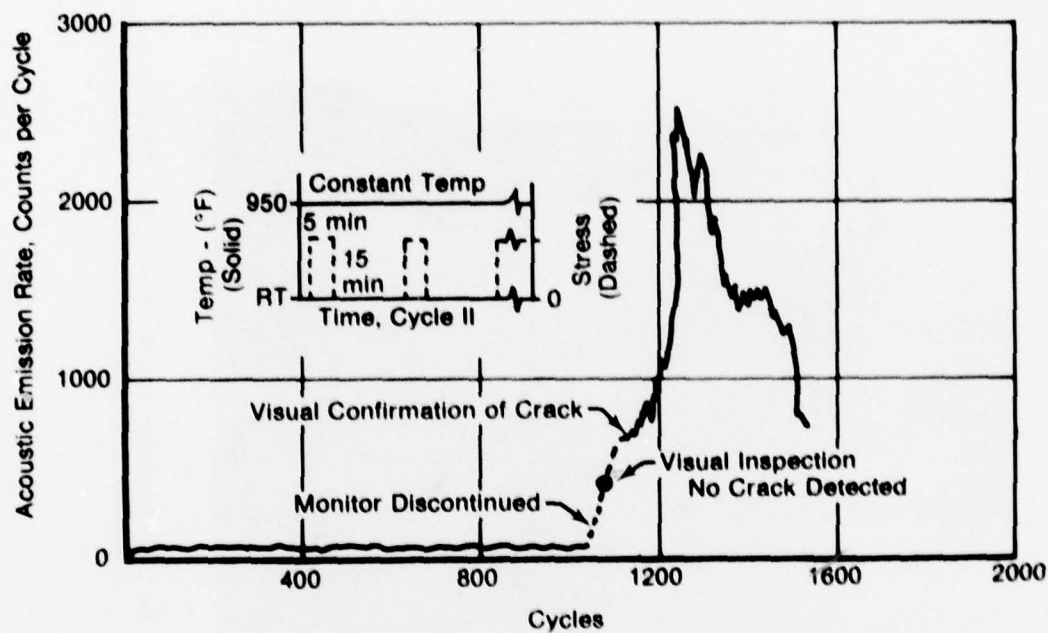
Figure 13. *Acoustic Emission Rate Monitor HSSC Bolthole Specimen No. 5786, Ti-6-2-4-2, Cycle II, 25 ksi Maximum*
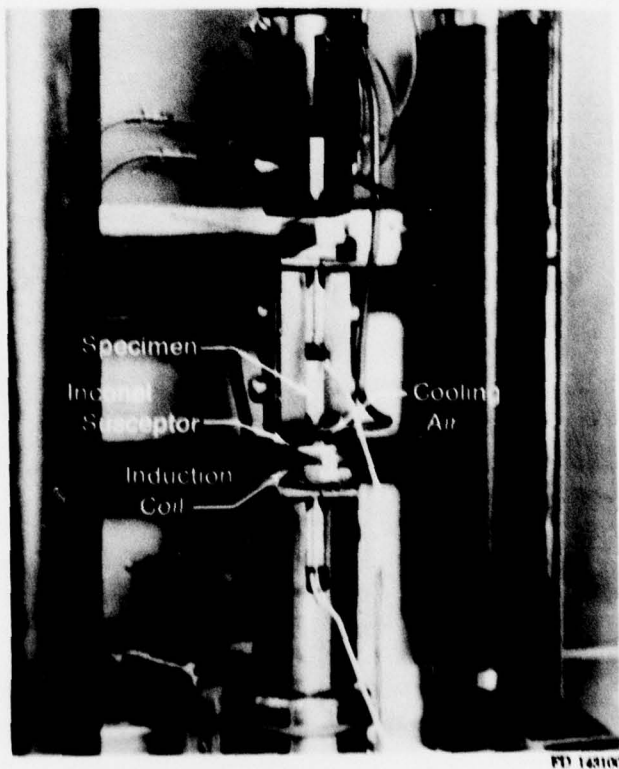
Figure 14. *Typical Two-Specimen Test Setup Using Induction Heating*
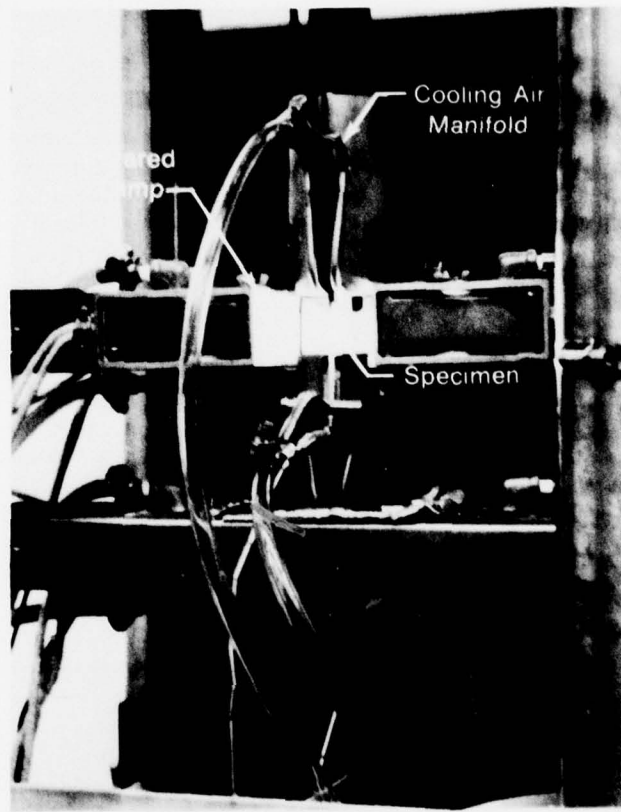
20

Figure 15. *Typical Infrared Lamp-Heated Two-Specimen Test Setup Showing Side Reflector Removed from Upper Assembly*

SECTION VI

TEST RESULTS

PHASE I

Phase I testing of beta processed Ti-6-2-4-2 material established the cyclic HSSC characteristics for eight different thermal-mechanical cycle configurations using a simulated takeoff temperature of 950°F. Results of Phase I testing are presented in Table 7 and in Figures 16 and 17. Figure 16 shows cyclic HSSC crack initiation life versus takeoff (maximum) stress for each cycle configuration tested. Figure 17 presents the same data as a function of accumulated time at takeoff temperature, or 950°F threshold stresses of each flight cycle. These curves allow a direct comparison of cyclic data with previously established static-load minibolthole data (Reference 6).

Tests performed at a constant 950°F temperature and a 5-min on/15-min off stress cycle (Cycle II) exhibited higher 100 hr threshold stress (cumulative test time at 950°F) than previously established (Reference 6) statically-stressed minibolthole specimens. These data tend to confirm observations by other investigators (Reference 5) that alternating either stress or temperature causes increases in threshold stress. Simultaneous cycling of stress and temperature by the Basic Cycle schedule (5-min takeoff + 5-min shutdown dwell) resulted in a twofold increase, compared to Cycle II (Figure 16), in the stress required to produce cracking at a given crack initiation life. Basic Cycle 100-hr threshold stress was approximately 2.5 times that of the static-stress miniboltholes as shown in Figure 17. This takeoff plus shutdown dwell simulation was the simplest thermal-mechanical cycle tested, and produced the greatest observed increase in crack initiation life.

Extension of the Basic Cycle takeoff dwell time from 5 to 15 min (Cycle IIIb) resulted in a decrease in initiation life compared to the Basic Cycle. However, threshold stress remained well above both cyclic-load and static-load isothermal threshold stresses (Figure 17).

The addition of the simulated idle and cruise components to the Basic Cycle (Cycles V, VI, and VII) produced no improvement in the Basic Cycle crack initiation life. Rather, based on the limited data, the addition of the other flight-cycle components might have resulted in a slight reduction in life.

Testing was performed to evaluate the effect of resalting on the HSSC characteristics of the Basic Cycle. Cycle III testing consisted of a stress/temperature dwell time profile which was identical with the Basic Cycle, and incorporated a periodic resalting at predetermined intervals. Cycle III results showed that resalting five times produced no significant effect on Basic Cycle HSSC crack initiation life 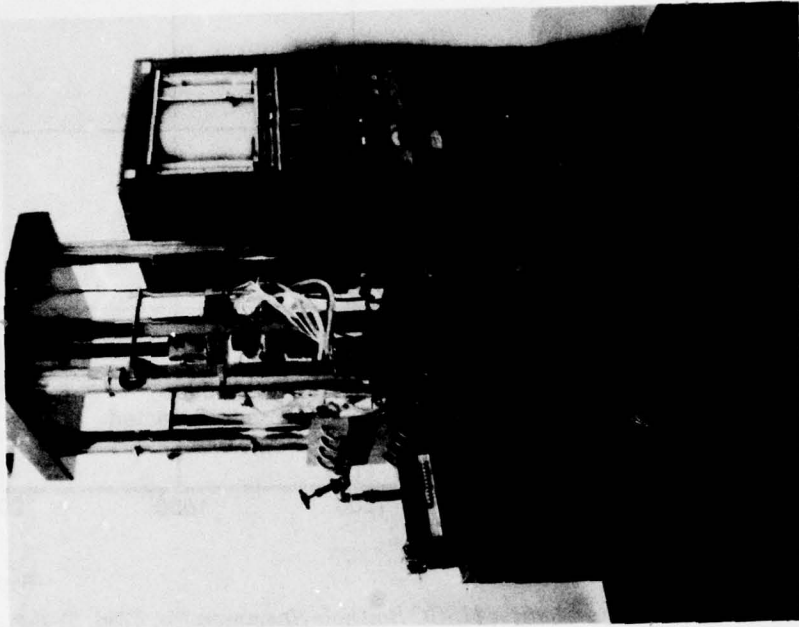at 45 ksi. Resalting once at a higher stress level of 55 ksi produced a possible reduction in life. However, only two data points were used to define the Cycle III crack initiation curves, and the apparent reduction in life could be attributed to normal data scatter.

The effect of a simulated hot shutdown dwell was investigated using Cycle VIII, which consisted of a 5-min dwell at takeoff temperature (950°F) and stress followed by a 15-min dwell at reduced temperature (200°F) and stress. This hot shutdown dwell component was for simulation of a short stop between flights where the heat soak-back during shutdown maintains some intermediate temperature. The hot shutdown dwell had no significant effect on the Basic Cycle crack initiation life.

TABLE 7. PHASE I HSSC TEST RESULTS FOR BETA-PROCESSED Ti-6-2-4-2 BOLTHOLE SPECIMENS SUBJECTED TO VARIOUS MISSION CYCLES AT 950°F TAKEOFF TEMPERATURE

Cycle Type	Temperature/Stress Profile	Specimen No.	Stress — ksi			Duration of Test		Remarks
			Idle	Takeoff	Cruise	No. of Cycles	Cum hr at 950°F	
Basic Cycle		5780	—	29.0	—	1200	100	No cracks
		5764	—	32.6	—	1200	100	No cracks
		5752	—	36.5	—	1200	100	No cracks
		5732	—	40.0	—	1200	100	No cracks
		5778	—	40.0	—	5625	469	HSSC cracks
		5761	—	45.0	—	1200	100	No cracks
		5750	—	50.0	—	2489	207	HSSC cracks
		5729	—	55.0	—	1200	100	No cracks
		5789	—	62.2	—	144	12	HSSC cracks
		5765	—	70.0	—	52	4.3	HSSC cracks
II		5777	—	20.0	—	300	100	No cracks
		5749	—	25.0	—	300	100	No cracks
		5786	—	25.0	—	1145	381	HSSC cracks
		5762	—	30.0	—	300	100	HSSC cracks
		5730	—	36.0	—	300	100	HSSC cracks
		5782	—	40.0	—	314	104.7	HSSC cracks
III (Resalt)		5790	—	45.0	—	2880	240	HSSC cracks
		5758	—	55.0	—	200	16.7	HSSC cracks
IIIb		5748	—	40.0	—	613	153.0	No cracks
		5770	—	45.0	—	152	38.0	HSSC cracks
		5736	—	55.0	—	19	4.75	HSSC cracks
V		5783	15.0	40.0	—	2362	196.8	HSSC cracks
		5779	15.0	40.0	—	1200	100	HSSC cracks
		5763	16.9	45.0	—	1200	100	HSSC cracks
		5772	16.9	45.0	—	1299	108.25	HSSC cracks
		[1]5751	18.7	50.0	—	[1]750	62.5	HSSC cracks
		[2]5731	20.6	55.0	—	[2]500	41.6	HSSC cracks
		5733	20.6	55.0	—	285	23.75	HSSC cracks
VI		5787	15.0	40.0	36.4	1839	153.25	HSSC cracks
		5767	16.9	45.0	41.0	1121	93.4	HSSC cracks
		5753	19.1	51.0	46.4	219	18.25	HSSC cracks
VII		5788	15.0	40.0	36.4	2206	183.8	No cracks
		5745	18.7	50.0	45.5	544	45.3	HSSC cracks
		5757	18.7	50.0	45.5	206	17.2	HSSC cracks
		5738	20.6	55.0	50.0	424	35.3	HSSC cracks
		5741	20.6	55.0	50.0	649	54.0	HSSC cracks
VIII[3]		5769	—	45.0	—	2583	215.2	HSSC cracks
		5739	—	55.0	—	671	55.9	HSSC cracks

[1]Large crack present at 750 cycles. Accurate initiation life is not known.
[2]Complete failure occurred at 500 cycles. Initiation life is not known. HSSC was indicated.
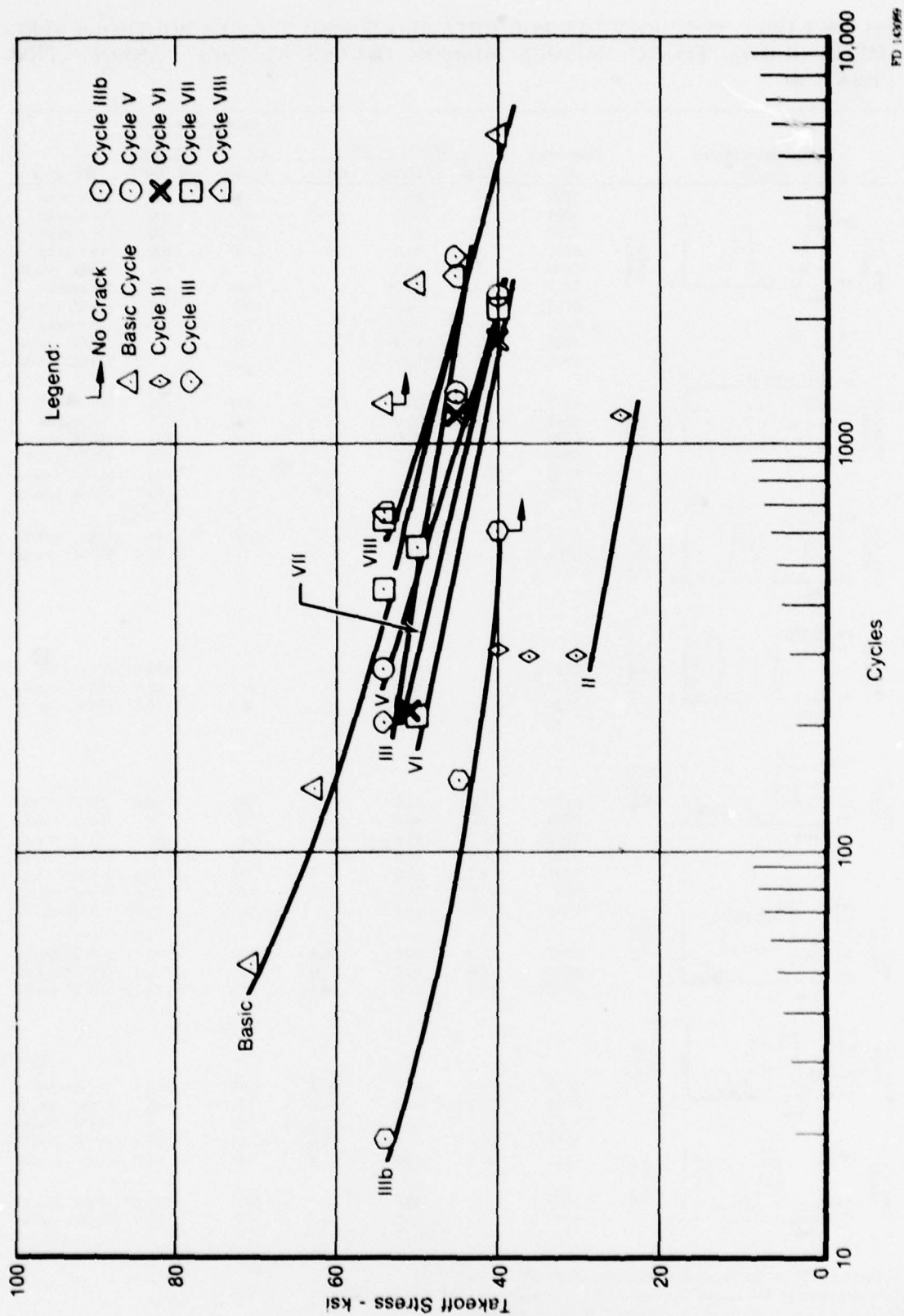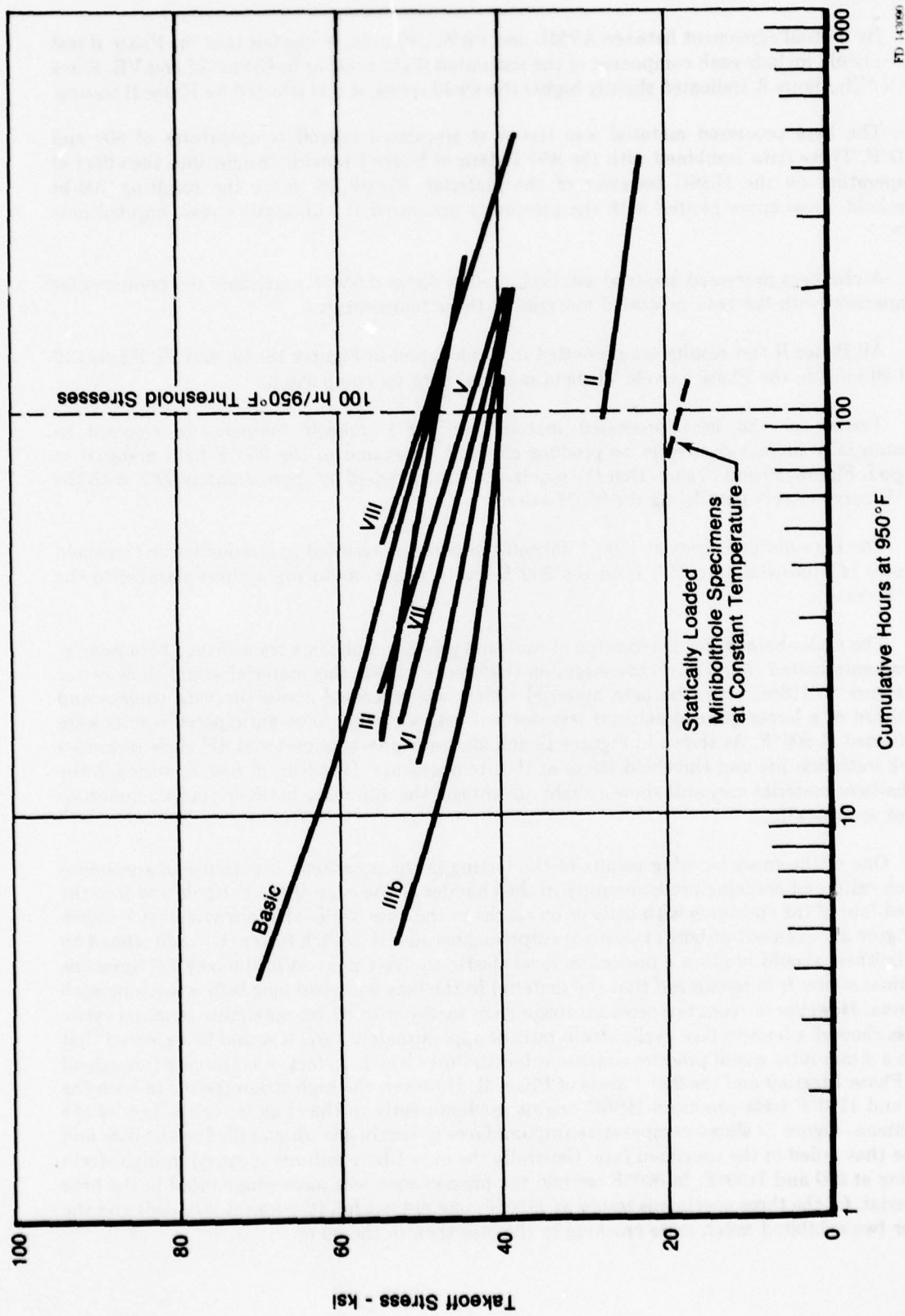[3]Cycle VIII 200°F shutdown stress = 37.5% of takeoff (maximum) stress.

Figure 16. Phase I HSSC Crack Initiation Curves

24

FD 143959

Figure 17. Phase I 950°F HSSC Threshold Stresses

PHASE II

By mutual agreement between AFML and P&WA/Florida, it was felt that the Phase II test cycle should include each component of the simulated flight cycle as in Cycles VI and VII. Since Cycle VII, Figure 8, indicated slightly higher threshold stress, it was selected for Phase II testing.

The beta processed material was tested at simulated takeoff temperatures of 800 and 1100°F. These data combined with the 950°F data of Phase I provide insight into the effect of temperature on the HSSC behavior of the material. Figure 18 shows the resulting 100-hr threshold stress curve plotted with the previously generated 100 hr, static stress, minibolthole data.

Alpha-beta processed material was evaluated at 800 and 950°F maximum temperatures for comparison with the beta processed material at those temperatures.

All Phase II test results are presented in Table 8 and in Figures 18, 19, and 20. Figures 19 and 20 include the Phase I Cycle VII beta material data for comparison.

Testing of the beta processed material at 800°F takeoff temperature resulted in substantially increased stresses to produce cracking compared to the 950°F beta material of Phase I. Figures 19 and 20 show that the required stress increased by approximately 50%, with the 800°F curve closely paralleling the 950°F curve.

The beta material tests at 1100°F takeoff temperature resulted in a reduction in threshold stresses of approximately 25% from the 950°F levels, again producing a curve parallel to the 950°F curve.

The alpha-beta material consisted of equiaxed primary alpha in a transformed beta matrix. It was anticipated from Gray's investigation (Reference 7) that this material would show better resistance to HSSC than the beta material which was processed above the beta transus and consisted of a larger grained acicular transformed beta structure. The anticipated results were confirmed at 800°F. As shown in Figures 19 and 20, the alpha-beta material did show increased crack initiation life and threshold stress at that temperature. However, at 950°F, although the alpha-beta material may still show a slight advantage, the difference between the two materials is not so dramatic.

One of the most puzzling results of the testing is the occasional occurrence of specimens which exhibited cracking predominantly in the chamfer at the edge of the bolthole and into the salted face of the specimen with little or no cracks in the bore itself. This phenomenon is shown in Figure 21. Such out-of-bore cracking is surprising because the notch factor ($K_t = 2.5$) offered by the bolthole should produce a maximum local elastic equivalent stress in the bore 2.5 times the nominal stress. It is recognized that the material in the bore will yield long before reaching such a stress. However, a room temperature strain gage survey with 80 ksi maximum nominal cyclic stress showed a bore-to-face cyclic strain ratio of approximately 1.37. It would be expected that such a strain ratio would produce consistent bore failures which, in fact, was the case through all the Phase I testing and the 950°F tests of Phase II. However, the high strain testing in both the 800 and 1100°F tests produced HSSC origins predominantly in the chamfer or the face of the specimen. Figure 22 shows comparative fracture faces of specimens which failed in the bore and those that failed in the specimen face. Generally the out-of-bore failures occurred in high strain testing at 800 and 1100°F. In 800°F testing, the phenomenon was more pronounced in the beta material. Of the three specimens tested at 1100°F, one did not fail (the lowest strained) and the other two exhibited much more cracking in the face than in the bore.

TABLE 8. PHASE II HSSC TEST RESULTS FOR Ti-6-2-4-2 BOLTHOLE SPECIMENS SUBJECTED TO CYCLE VII TEST CONDITIONS

| Specimen No. | Structure | Takeoff Conditions | | Duration of Test | | Remarks |
		Temperature (°F)	Stress (ksi)	No. of Cycles	Cum Time at Takeoff (hr)	
5768	beta	800	63.0	1,268	105.7	HSSC cracks
5747	beta	800	70.0	932	77.7	HSSC cracks
5742	beta	800	77.5	201	16.7	HSSC cracks
5784	beta	1100	29.0	1,730	144.2	No cracks
5746	beta	1100	36.0	328	27.3	HSSC cracks
5735	beta	1100	40.0	259	21.6	HSSC cracks
5775	alpha-beta	800	71.0	675	56.2	HSSC cracks[1]
5791	alpha-beta	800	80.0	772	64.3	HSSC cracks[1]
5743	alpha-beta	800	85.0	301	25.1	HSSC cracks[2]
5744	alpha-beta	800	85.0	340	28.3	HSSC cracks[2]
5776	alpha-beta	950	45.0	1,284	107.0	HSSC cracks
5759	alpha-beta	950	55.0	887	73.9	No cracks
5792	alpha-beta	950	61.0	26	2.2	HSSC cracks

[1] Cleavage initiations were extremely shallow (~0.001 in.) with crack progression by fatigue.

[2] Cleavage initiations were shallow (~0.005 in.) with crack propagation by a fatigue/cleavage combination.
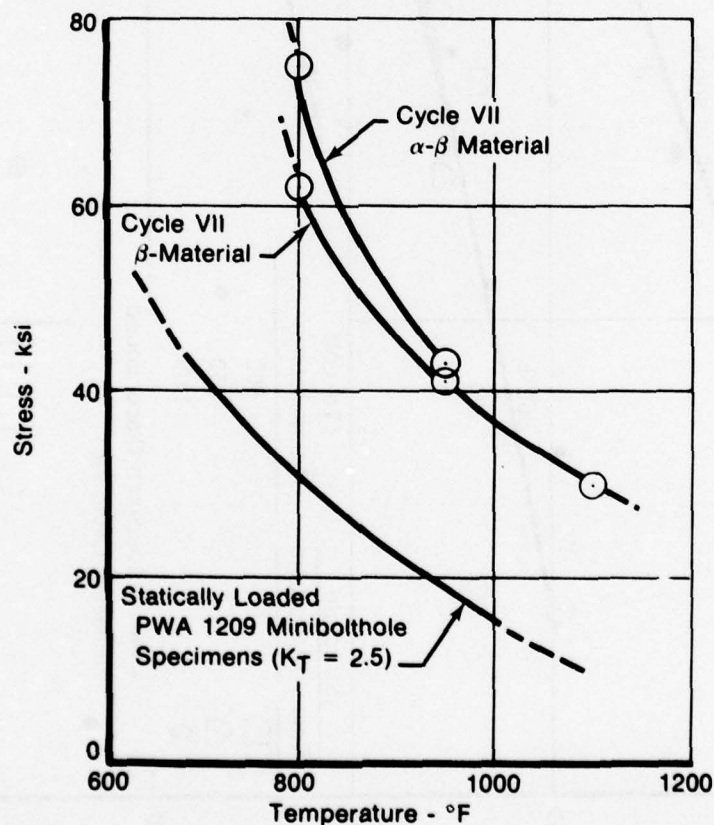
FD 143091

Figure 18.   Ti-6-2-4-2 Hot Salt Stress Corrosion 100-Hour Threshold Stress Curves

27
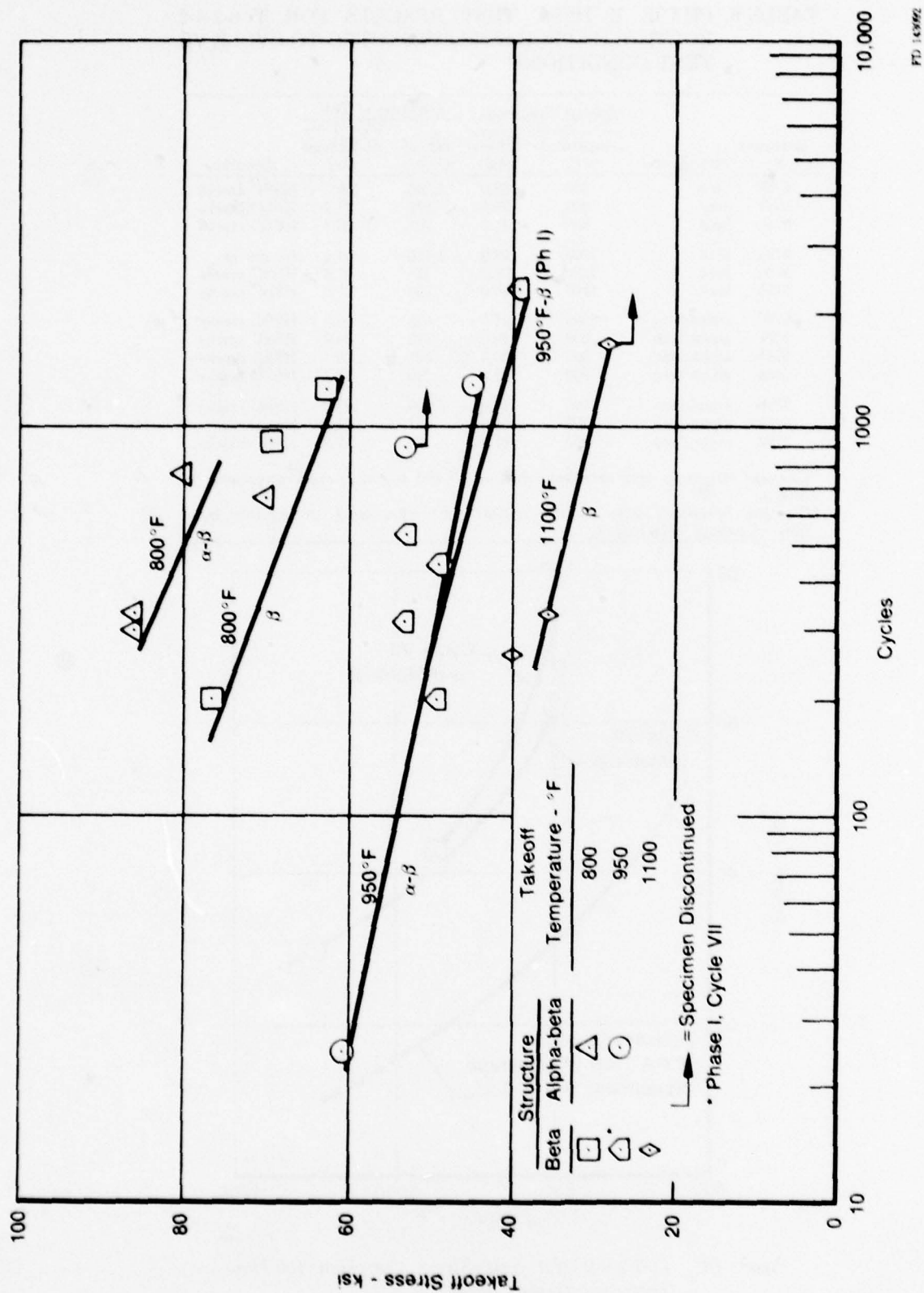
Figure 19. *Phase II HSSC Crack Initiation Curves*

28
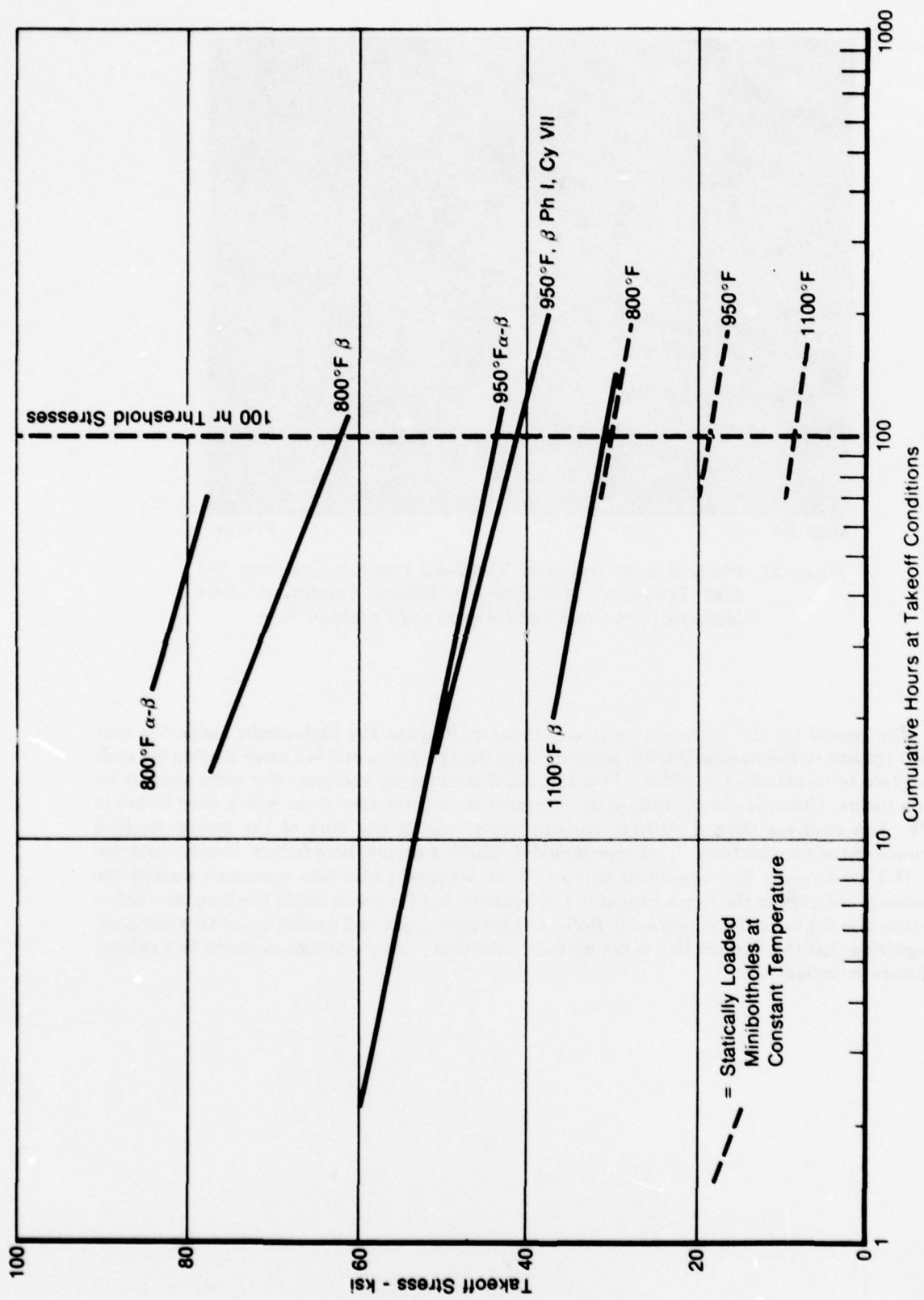
Figure 20. Phase II Threshold Stress Curves

29

PD 143966
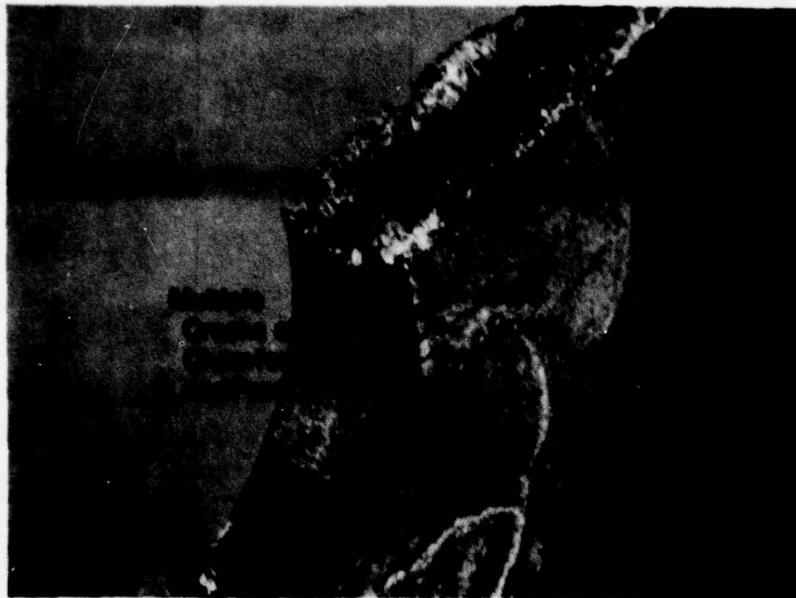
Mag: 6X   FD 137998

Figure 21. Phase II Beta Processed Ti-6-2-4-2 Bolthole Specimen No.
5746 Tested at 1100°F/36 ksi Takeoff Conditions. Note
Multiple Face Cracks and Absence of Cracks in Bore

The reason for the phenomenon is still unclear. Perhaps the high strain inside the bore caused the salt to mechanically spall, separate from the specimen, and fall away leaving the still-salted face to be attacked by HSSC. Post-test SEM microprobe analyses offer some support for such a theory. Chloride concentrations were measured on three specimens which were tested at 800°F. The analyses showed definite chloride remaining in the bore of the lowest strained specimen of the beta material. This specimen did exhibit a normal bore failure. Similar analyses of a 77.5 ksi stressed beta specimen and an 85 ksi stressed alpha-beta specimen showed the presence of chloride on the face adjacent to the bolthole, but the levels inside the bore were below the detection limits of the microprobe. Both of these specimens had predominant face cracking. Recognizing that this explanation is not without limitation, this phenomenon might be a subject for future investigations.

Mag: 3X
A. Beta Specimen No. 5738, Cycle VII, 950°F Takeoff
Temperature, Crack Origins Inside Bore

FAL 46817
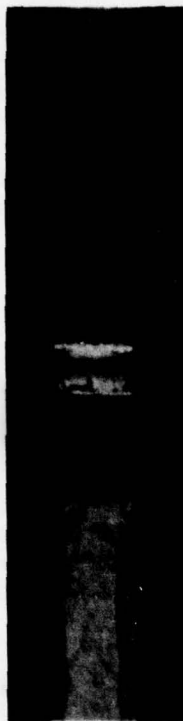
Mag: 3X
C. Alpha-Beta Specimen No. 5776, Cycle VII, 950°F
Takeoff Temperature, Crack Origins Inside Bore

FAL 47368

Fig. 35A

Mag: 3X
B. Beta Specimen No. 5747, Cycle VII, 800°F Takeoff
Temperature, Crack Origins at Face and Chamfer

FAL 47367

Fig. 35B

Mag: 4X
D. Alpha-Beta Specimen No. 5743, Cycle VII, 800°F Takeoff
Temperature, Crack Origins Inside Bore and on Face

FAL 48215

FD 143964

Figure 22. Ti-6-2-4-2 HSSC Bolthole Specimen Crack Origins

31

FRACTOGRAPHIC ANALYSIS

The fracture morphology of the failed specimens in this program were generally characterized by three steps: (1) corrosion-produced intergranular crack initiation, (2) cleavage-type propagation, and (3) dimple rupture resulting from the room temperature tensile rupture of the specimen. The SEM analysis of one specimen was particularly useful in demonstrating various features of the fracture morphology produced by this program. The specimen was No. 5782, subjected to the Cycle II test conditions. This particular specimen was unique in that the testing was continued for 321 cycles after crack initiation was detected at which point it was tensile ruptured at room temperature.

Figure 23 shows an overall view of the fracture face with locations of subsequent morphological features indicated. Figures 24 through 29 show: (1) corrosion products of HSSC crack initiation — Figure 24, (2) brittle cleavage propagation — Figure 25, (3) transition between cleavage mode and fatigue — Figure 26, (4) fatigue propagation — Figures 27 and 28, and (5) dimple rupture — Figure 29. An SEM microprobe analysis (Table 9) shows chloride concentration by weight-percent at the various locations shown in Figures 24 through 27.

In a few cases, SEM analysis showed "islands" of fatigue within the brittle cleavage-type fracture zone. Figure 30 shows one example. This phenomenon is particularly interesting because it implies that during the course of the test, the rapid, brittle, cleavage-type propagation was arrested only to be resumed again after a period of relatively slow propagation of the crack by fatigue.

B. F. Brown (Reference 8) relates instances of having seen similar "islands" of dimple rupture morphology amidst cleavage zones in fracture faces of statically loaded salt stress corrosion specimens. Briefly, his explanation states:

> There appears to be a threshold stress intensity for a given material/corrodant system below which HSSC is not observed. This has come to be known as K_{Iscc}. Crack initiation is induced by corrosion. As the stress intensity increases above K_{Iscc}, given the other conditions necessary for HSSC, fracture is almost entirely cleavage. Should the stress corrosion mechanism be interrupted, the stress intensity will increase and approach K_{Ic} producing areas of dimple rupture. Assuming the conditions for HSSC are restored, the cleavage mode of propagation is continued. "Thus the overall cracking process is a dual one in which a mechanochemical fracturing process is interspersed with islands of purely mechanical fracturing."

There has been some question concerning the conditions under which the cleavage zone is produced. Mahoney and Tetelman (Reference 9) have suggested that the absence of corrosion products in the cleavage zone indicates that the cleavage occurred during the ambient temperature rupture of the specimen required to reveal the fracture face. However, the areas of fatigue surrounded by cleavage, produced in this program, prove that the cleavage fracture morphology is a result of the elevated temperature cyclic loading part of the test.

Typical HSSC damage penetration measurements for the various Phase I thermal-mechanical cycles tested are compared in Figure 31. The deepest corrosion penetration was observed on a high stress (55 ksi) Cycle IIIb extended dwell specimen, which also exhibited the lowest crack initiation life (19 cycles). Corrosion penetration for Cycle IIIb at lower stress was comparable to other cycles.

The SEM examination of fracture surfaces of Phase II beta specimens showed, as in Phase I, a predominance of cleavage at the origins. Typical fracture origins of beta material, tested at 800 and 1100°F takeoff temperatures, are shown in Figure 32. Depth of cleavage penetrations ranged from 0.015 to 0.030 in. These cleavage fracture features were similar to those of the 950°F Phase I tests.

32
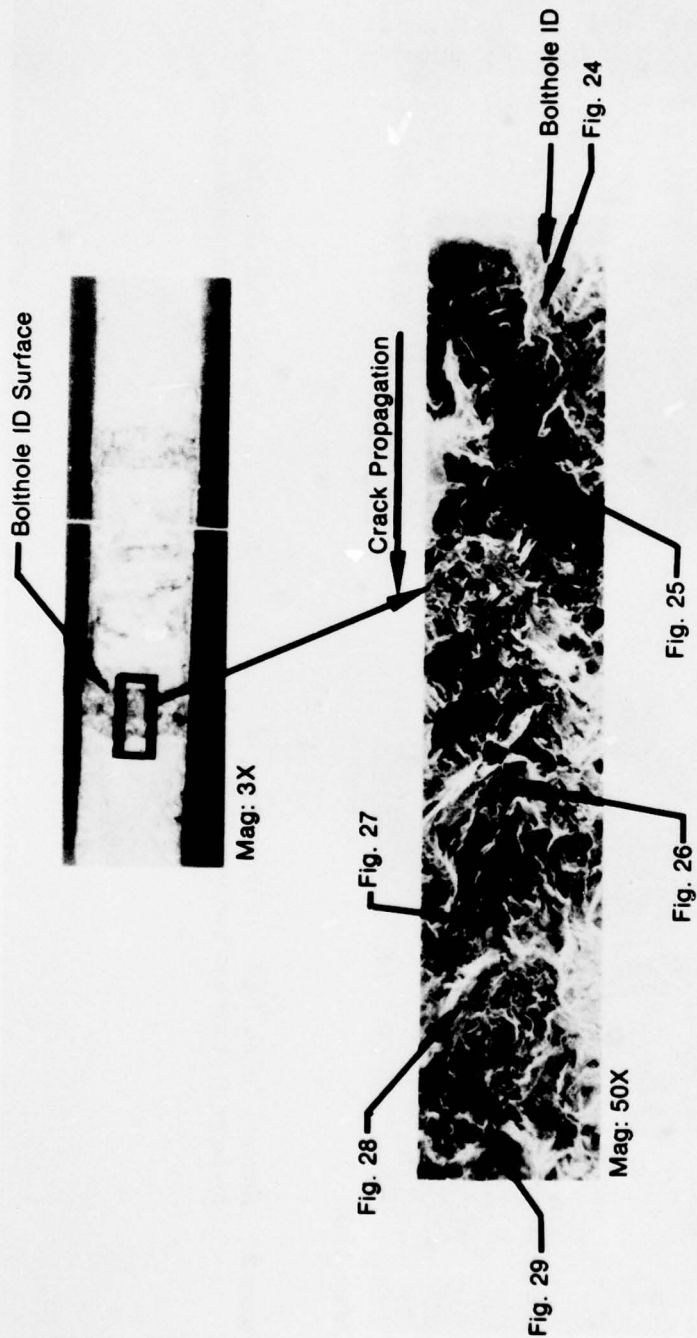
Figure 23. Photomicrograph of Typical Stress Corrosion Initiated Fracture Face of β-Processed Ti-6-2-4-2 Bolthole Specimen No. 5782 After Cycle II Testing at 40 ksi Maximum Stress for 635 Cycles

33

Mag: 500X

FAM 07762

FD 11196

Figure 25. *Fracture Following Origin Showing Typical Cleavage Type Failure Mode*

Mag: 500X

FAM 07763
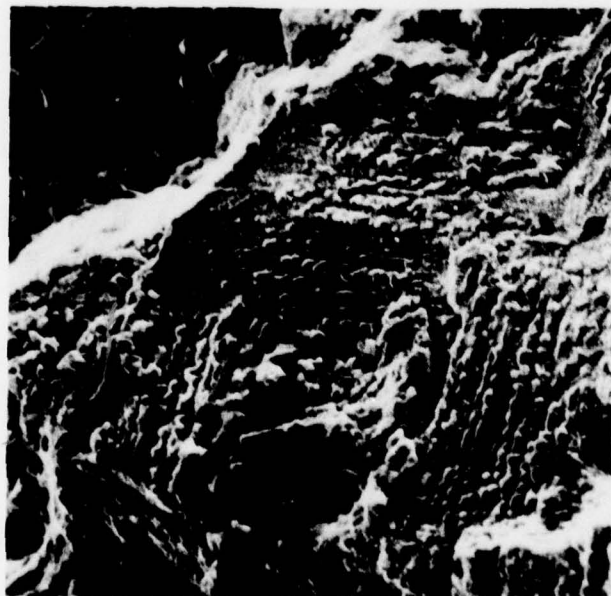
FD 11197

Figure 24. *Fracture Origin With Features Obscured by Layer of Oxide and Corrosion Products*

34
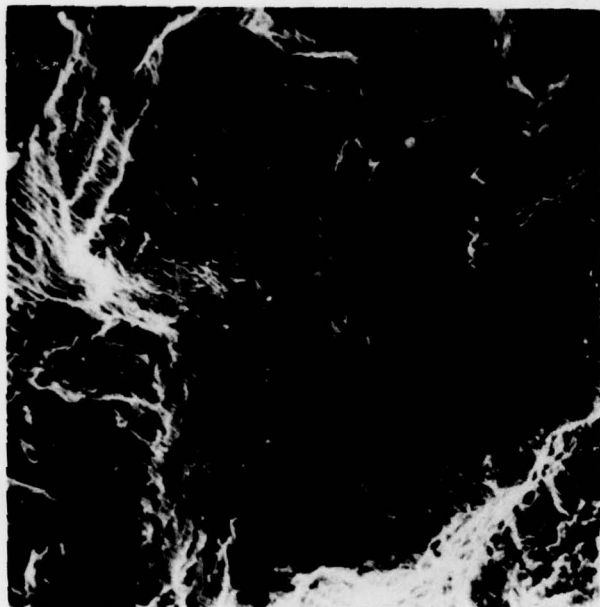
Mag: 500X

FAM 87561

FD 11979

Figure 27. Typical Fatigue Following the Area of Transition from Cleavage to Fatigue

Mag: 500X

FAM 87550

FD 11978

Figure 26. Transition from Cleavage Mode (Lower Right) to Fatigue (Upper Left)

35

FAM 87546

FD 111961

Mag: 500X

Figure 29. Section of the Specimen Opened in the Room Temperature Tensile Mode After the Termination of Cycle II Testing
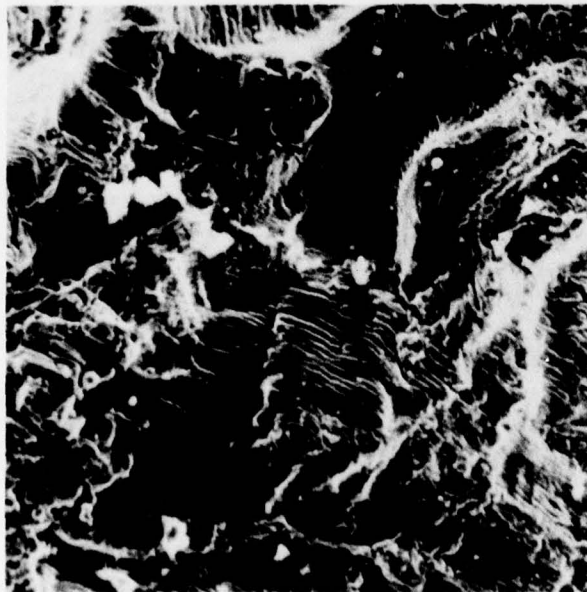
FAM 87549

FD 111960

Mag. 500X

Figure 28. Typical Fatigue Near End of Crack Penetration

TABLE 9. CHLORINE CONCENTRATIONS AT VARIOUS CRACK PENETRATION DEPTHS FOR Ti-6-2-4-2 SPECIMEN NO. 5782 AFTER 635 CYCLES (211.7 hr) UNDER CYCLE II CONDITIONS

Crack Penetration Depth (in.)*	Weight Chloride (%)	Fracture Surface Description
0	1.03	Corrosion Products and Cleavage
0.010	0.96	(Figure 24)
0.020	0.21	Cleavage (Figure 25)
0.030	0.16	
0.040	0.12	Cleavage/Fatigue Transition
0.050	0.10	(Figure 26)
0.060	0.07	
0.070	0.05	Fatigue (Figure 27)
0.080	0.05	

* Depth of crack penetration measurements were from a section taken at the center of the specimen thickness.

Mag: 500X   FAM 88439

c. Fatigue Area in Cleavage
    Fracture Zone

Mag: 500X   FAM 88438

b. Fatigue Area in Cleavage
    Fracture Zone

Mag: 50X   FAM 88437
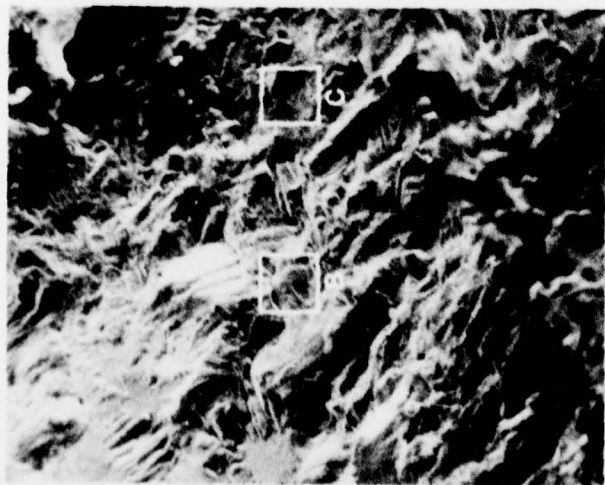
a. Fracture Surface with Cleavage
    Penetration to 0.050 in.
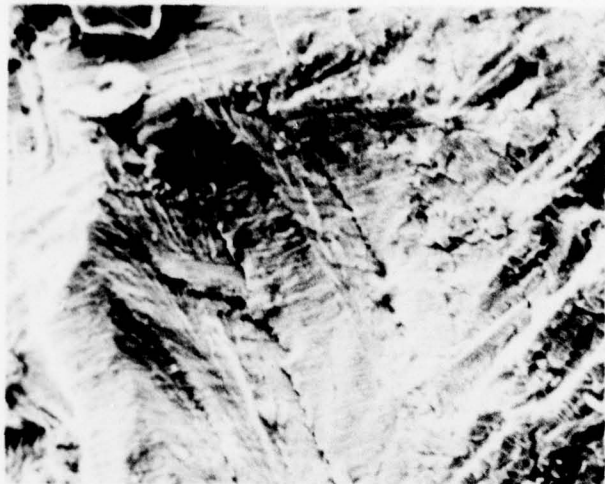
Figure 30. Basic Cycle Specimen No. 5750 After 2489 Cycles, Tested at 950°F/50 ksi Takeoff Conditions

38

Note: Some Specimens on this Chart Were
Checked after Testing for Several Cycles
Beyond Crack Initiation. These Are Noted
by Number of Cycles Total and No. of
Cycles to Initiation

FD 143995

VIII
5 min
Load and
Temp
671 Cy — 55 ksi
2583 Cy — 45 ksi

VII
5 min
Load and
Temp
649 Cy — 55 ksi
424 Cy — 55 ksi
544 Cy — 50 ksi
206 Cy — 50 ksi

VI
5 min
Load and
Temp
219 Cy — 51 ksi
1121 Cy — 45 ksi
1839 Cy — 40 ksi

V
5 min
Load and
Temp
285 Cy — 55 ksi
1299 Cy — 45 ksi
2362 Cy — 40 ksi

IIIb
15 min
Load and
Temp
19 Cy — 55 ksi
186 Cy — 45 ksi

III
5 min
Load and
Temp
200 Cy — 55 ksi
2880 Cy — 45 ksi

II
5 min Load
Constant
Temp
635 Cy Total (314 Cy Init) — 40 ksi

Basic
5 min
Load and
Temp
71 Cy Total (52 Cy Init) — 70 ksi
211 Cy Total (144 Cy Init) — 62 ksi
2489 Cy — 50 ksi

0.100
0.080
0.060
0.040
0.020
0

Cleavage Penetration Depth - in.

Takeoff { Stress {
Cycle Type { Takeoff { Dwell

Figure 31. HSSC Crack Penetration Chart For Typical Phase I Ti-6-2-4-2 Bolthole Specimens

39

Mag: 500X

FAM 88793

B. Specimen No. 5746, Tested at
1100°F/36 ksi Takeoff Conditions

FD 143946

Mag: 500X

FAM 88792

A. Specimen No. 5768, Tested at
800°F/63 ksi Takeoff Conditions

Figure 32. Beta Material HSSC Fracture Surfaces

40

Alpha-beta material tested at 950°F also displayed cleavage morphology near the fracture origin. However, this feature of the smaller grained material is not as distinctive as with the beta-processed material. The SEM micrographs in Figures 33 and 34 indicate the similarity between cleavage and dimple rupture. Cleavage crack penetration depths of 0.015 to 0.020 in. were observed.

The observation from cyclic HSSC test results that alpha-beta material shows better resistance to HSSC than beta material at 800°F is supported by SEM comparisons of fracture surfaces of the two microstructures. Figure 35 shows relative penetrations of cleavage for beta and alpha-beta material tested at 800°F takeoff temperature. Figure 35A, a beta material fracture origin, clearly shows cleavage visible at only 50X magnification. The fracture morphology was all cleavage to a depth of approximately 0.030 in. Cleavage penetration in an alpha-beta material fracture (Figure 35B) was approximately 0.003 in. (10% of the beta penetration) followed by a combination cleavage/fatigue crack propagation mode. Figure 35C.

CHLORIDE ION ANALYSIS

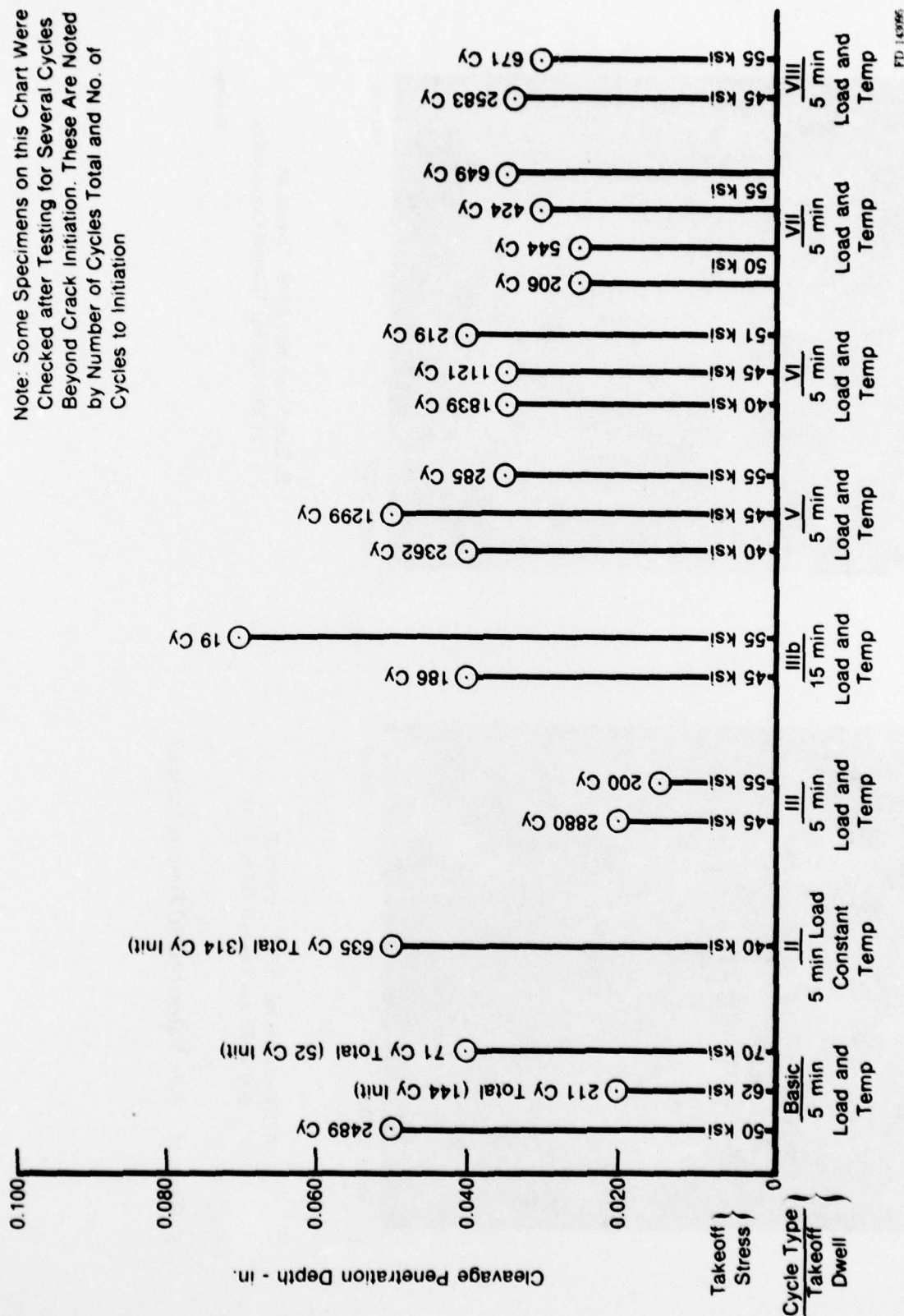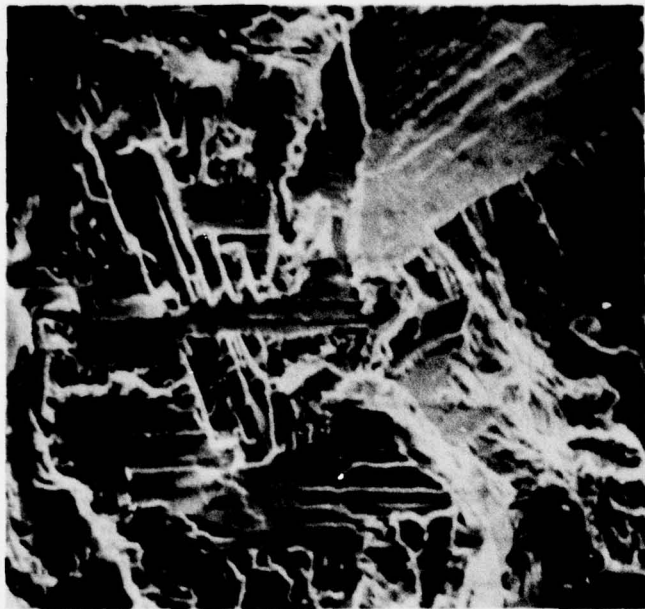Initially in the program, both pretest and post-test salt concentrations were expressed in terms of weight of sea salt solids per unit area of salted surface. The method of expressing salt concentration in this manner was later changed in favor of a direct expression of residual chloride rather than total solids. This change was instituted when it was discovered that the previous practice of converting residual chlorides to assumed sea salt solids (by weight ratio) was not accurate for post-test concentrations. A post-test quantitative analysis for residual sodium on a long-term Cycle VI test showed that most of the sea salt solids remained on the specimen during the test. However, a similar analysis for residual chloride on the same specimen showed that a severe depletion of water soluble chloride had occurred during the test. The pretest weight ratio of soluble chloride to sea salt solids was substantially reduced during testing, therefore, it was unsuitable for determining post-test concentrations.

Chloride concentrations, as determined by specific ion electrode, were recorded prior to and after each test. These concentrations are presented in Tables 10 (Phase I) and 11 (Phase II). The pretest concentrations were calculated based on measurements obtained from a control sample which was salted at the same time as the test specimen. Post-test chloride concentration measurements were obtained from specimens immediately after cyclic testing.
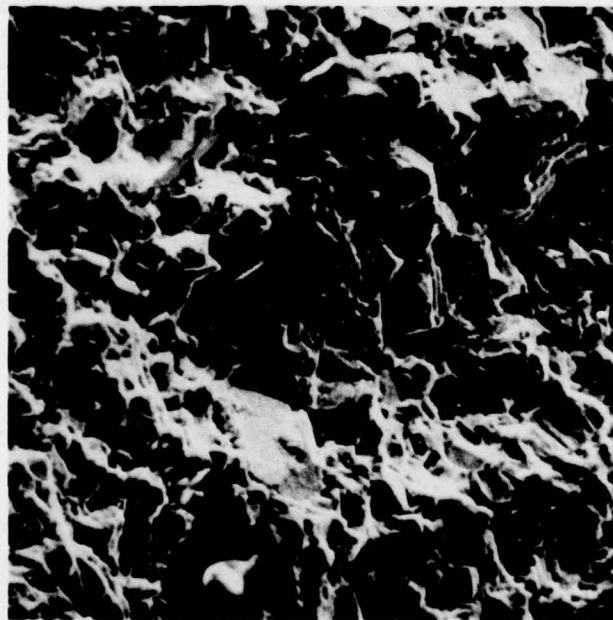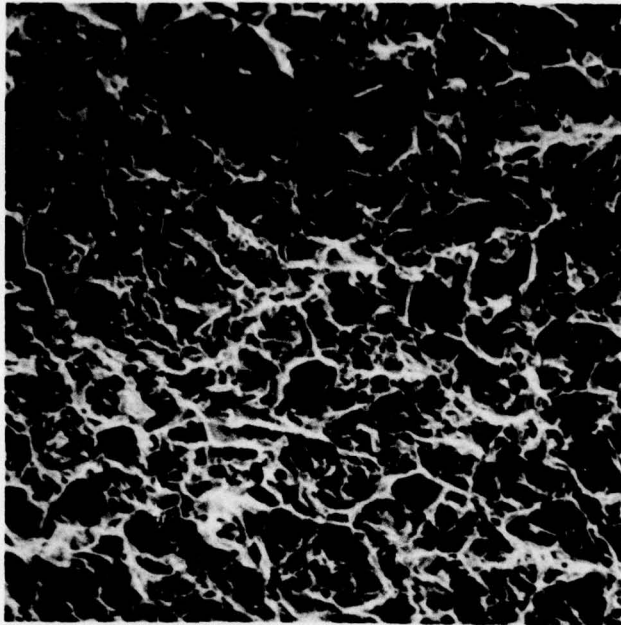
FAM 88798

FD 143987

Mag: 500X

B. Appearance of Overstress Area
(Room Temperature Tensile Failure)

FAM 88799

Mag: 500X

A. Appearance of Cleavage in HSSC Area

Figure 33. SEM Photographs of Fracture Features of Alpha-Beta Specimen No. 5776 Tested at 950°F/45 ksi Takeoff Conditions

42

Mag: 2000X   FAM 88797

A. Appearance of Cleavage in HSSC Area
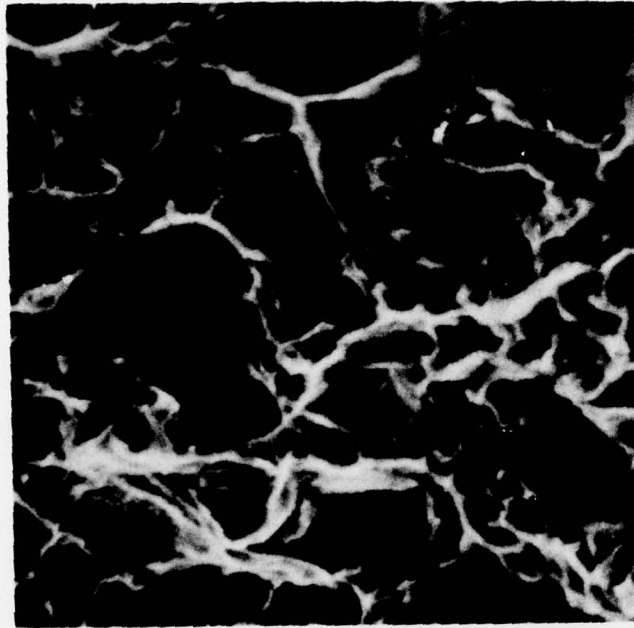
FAM 88796

Mag: 2000X   B. Appearance of Overstress Area
(Room Temperature Tensile Failure)

FD 14309R

Figure 34. *SEM Photographs of Fracture Features of Alpha-Beta Specimen No. 5776 Tested at 950°F/45 ksi Takeoff Conditions*

43
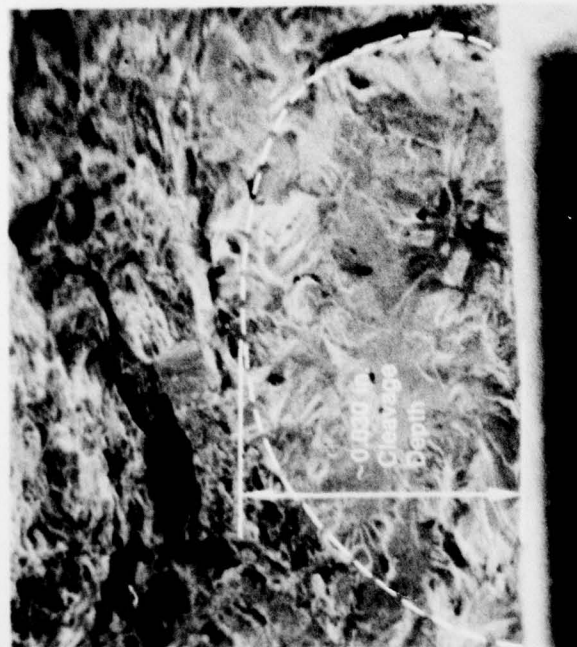
Mag: 50X

Mag: 50X

Mag: 500X

A. Beta Specimen No. 5747
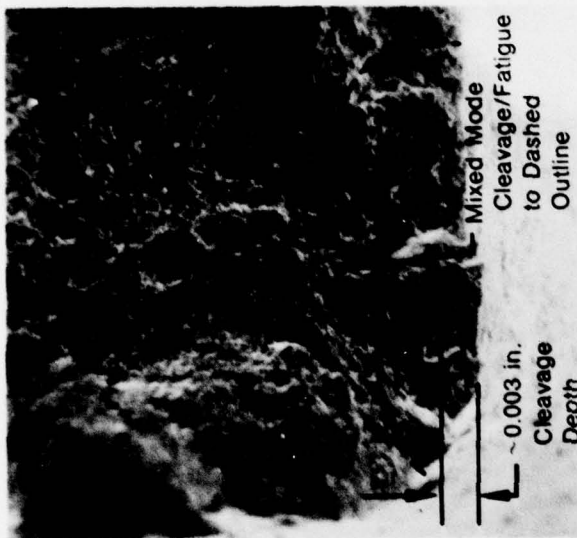
B. Alpha-Beta Specimen No. 5743

C. Alpha-Beta Specimen No. 5743
   Cleavage to Cleavage/Fatigue
   Transition Area

Figure 35. Fracture Features of a Beta and an Alpha-Beta Specimen, Both Tested At 800°F Takeoff Temperature, Cycle VII

44

TABLE 10. PHASE I CHLORIDE ANALYSES RESULTS FOR HSSC TESTING OF BETA-FORGED Ti-6-2-4-2 BOLTHOLE SPECIMENS

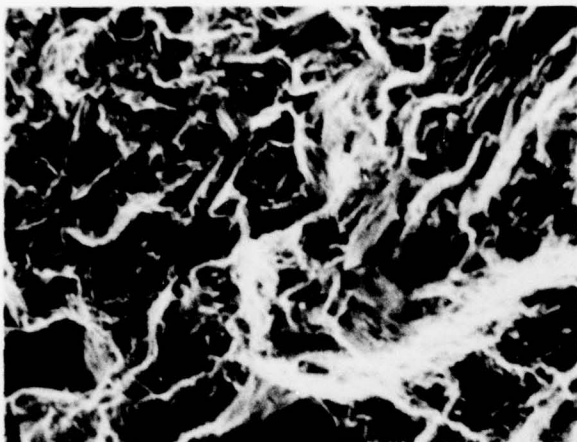| Specimen No.	Cycle Type	Maximum Stress (ksi)	Duration of Test		Cloride Concentration (mg/in.²)	
			No. of Cycles	Cum Hr at 950°F	Pretest[1]	Post-test
5780	Basic	19.0	1200	100	~0.25	Not checked
5764	Basic	32.6	1200	100	~0.25	Not checked
5752	Basic	36.5	1200	100	~0.25	Not checked
5732	Basic	40.0	1200	100	~0.25	Not checked
5778	Basic	40.0	5625	469	[2]1.1	[2]0.04
5761	Basic	45.0	1200	100	~0.25	Not checked
5750	Basic	50.0	2489	207	[2]1.03	[2]0.03
5729	Basic	55.0	1200	100	~0.25	<0.01
5789	Basic	62.2	144	12	0.8	0.32
5765	Basic	70.0	52	4.3	0.99	0.41
5777	II	20.0	300	100	~0.25	Not checked
5749	II	25.0	300	100	~0.25	Not checked
5786	II	25.0	1145	381	0.76	0.33
5762	II	30.0	300	100	0.24	<0.01
5730	II	36.0	300	100	~0.25	Not checked
5782	II	40.0	314	104.7	2.32	0.24
5790	III	45.0	2880	40.0	1.09	[3]~0.15
5758	III	55.0	200	16.7	1.14	[4]0.87
5748	IIIb	40.0	613	153	0.85	0.31
5770	IIIb	45.0	152	38	0.85	0.05
5736	IIIb	55.0	19	4.75	0.99	0.99
5783	V	40.0	2362	196.8	1.28	0.04
5779	V	40.0	1200	100	~1.02	Not checked
5763	V	45.0	1200	100	~1.02	Not checked
5772	V	45.0	1299	108.25	1.32	0.07
5751	V	50.0	750	62.5	~1.02	Not checked
5731	V	55.0	500	41.6	~1.02	Not checked
5733	V	55.0	285	23.75	1.18	0.18
5787	VI	40.0	1642	153.25	1.18	[5]0.04
5767	VI	45.0	1121	93.4	1.18	<0.01
5753	VI	51.0	219	18.25	1.18	0.08
5788	VII	40.0	2206	183.8	1.09	0.04
5745	VII	50.0	544	45.3	1.09	0.07
5757	VII	50.0	206	17.2	1.06	0.23
5738	VII	55.0	424	35.3	1.09	0.10
5741	VII	55.0	649	54.0	1.25	0.15
5769	VIII	45.0	2583	215.2	1.13	0.04
5739	VIII	55.0	671	56.0	0.99	0.16

[1] To obtain pretest salt concentration, multiply pretest chloride by 2.115. This factor does not apply to post-test salt calculations; since the ratio of soluble chloride to sea salt solids diminishes with exposure time to test conditions.
[2] These chloride concentrations are exhibited after washing and resalting at 1200 cycles. Initial pretest concentration was ~0.25 mg/in.² for both specimens and was not checked at 1200 cycles.
[3] Specimen resalted 5 times during test.
[4] Specimen resalted once during test.
[5] Washed and resalted at 1642 cycles to 1.13 mg Cl⁻/in.² Test then continued to crack at 1839 cycles. Post-test analysis after crack showed 0.10 mg Cl⁻/in.²

TABLE 11. PHASE II CHLORIDE ANALYSES RESULTS FOR HSSC TESTING OF Ti-6-2-4-2 BOLTHOLE SPECIMENS UNDER CYCLE VII CONDITIONS

Specimen No.	Structure	Maximum Temperature (°F)	Maximum Stress (ksi)	Duration of Test		Chloride Concentration (mg/in.²)	
				No. of Cycles	Cum hr at Takeoff	Pretest[1]	Post-test
5768	beta	800	63.0	1268	105.7	0.94	0.15
5747	beta	800	70.0	932	77.7	0.85	0.04
5742	beta	800	77.5	201	16.7	1.24	0.18
5784	beta	1100	29.0	1730	144.2	0.94	0.04
5746	beta	1100	36.0	328	27.3	1.24	0.13
5735	beta	1100	40.0	259	21.6	1.04	0.05
5775	alpha-beta	800	71.0	675	56.2	1.12	[2]0.26
5791	alpha-beta	800	80.0	772	64.3	1.34	[2]0.27
5743	alpha-beta	800	85.0	301	25.1	1.21	Not checked
5744	alpha-beta	800	85.0	340	28.3	0.95	0.15
5776	alpha-beta	950	45.0	1284	107.0	1.56	0.03
5759	alpha-beta	950	55.0	887	73.9	1.04	0.016
5792	alpha-beta	950	61.0	26	2.2	1.27	[2]0.32

[1] To obtain pretest salt concentration, multiply pretest chloride by 2.115. This factor does not apply to post-test salt calculations, since the ratio of soluble chloride to sea salt solids diminishes with exposure time to test conditions.

[2] These specimens were broken in tension at room temperature prior to the post-test chloride analysis. One-half of each broken specimen was submitted for analysis by specific ion electrode.

SECTION VII

CONCLUSIONS

- Hot salt stress corrosion (HSSC) threshold stress for Ti-6-2-4-2 boltholes with isothermal cyclic loading showed a significant increase over that established by minibolthole isothermal static-load tests.

- HSSC threshold stresses for Ti-6-2-4-2 boltholes with simultaneous stress/temperature cycling showed dramatic increase over those established by isothermal cyclic-stress tests.

- Of the thermal-mechanical cycles tested, the Basic Cycle (a simple takeoff/shutdown dwell simulation) showed the highest threshold stress and crack initiation life.

- Extension of the Basic Cycle takeoff dwell from 5 to 15 min resulted in the lowest threshold stress and cyclic crack initiation life of the thermal-mechanical cycles tested.

- The addition of various simulated idle and cruise components to the Basic Cycle produced no significant effect on threshold stress or cyclic crack initiation life.

- The hot shutdown dwell (200°F/low-stress) of Cycle VIII produced no significant effect on Basic Cycle crack initiation life.

- Resalting had no apparent effect on crack initiation life.

- Beta material Cycle VII crack initiation life was increased when takeoff temperature was reduced from 950 to 800°F. There was approximately a 50% increase in stresses to produce a given life.

- Beta material Cycle VII crack initiation life was reduced with increased takeoff temperature from 950 to 1100°F. There was approximately a 25% decrease in stresses to produce a given life.

- At 800°F, the alpha-beta material exhibited higher cyclic crack initiation life than did the beta material.

- At 950°F, both the beta processed and alpha-beta material exhibited similar cyclic crack initiation life.

- Fracture surfaces of alpha-beta material subjected to cyclic thermal-mechanical testing at 800°F were characterized by shallow (0.001 to 0.005 in.) cleavage initiations followed by fatigue or a combination of cleavage/fatigue crack propagation.

SECTION VIII

RECOMMENDATIONS

Studies made possible by this contract have provided valuable insight into the nature of cyclic hot salt stress corrosion (HSSC) behavior. Results of the testing have also suggested certain other fields of investigation which would supplement these findings and provide additional impetus toward development of a life prediction system for engine components operating in HSSC environments. A list of suggestions for further investigations is:

1. Future studies should be planned to establish degradation in crack initiation life due to HSSC. These studies would require definition of baseline curves from unsalted specimens for comparison with cyclic HSSC data. To establish this relationship with a substantial degree of confidence it is essential that sufficient data points be planned to statistically substantiate resulting curves.

2. Since none of the flight components added to the Basic Cycle produced any significant increase in the cyclic crack initiation life, variations of a simple takeoff/shutdown simulation should be adopted for further cyclic HSSC investigations.

3. The standard strain-control specimen, FML 95716C (Figure 36), used by P&WA, Government Products Division should be investigated as a possible substitute for the bolthole specimen in cyclic HSSC life determinations. Strain-control specimen data have been shown to correlate with bolthole specimen results in standard LCF tests. It has also been used successfully to predict the life of cyclically-loaded engine components (disks) in the laboratory. The investigation of this strain-control specimen as a possible replacement for the bolthole specimen should include a strain survey of the bolthole and parallel thermal-mechanical tests of both types of specimens machined from the same forging. Adoption of the strain-control specimen would result in a substantial savings in material for future tests.

4. A minimum number of exploratory tests should be conducted to investigate the possibility of a threshold cyclic temperature.

5. Cyclic HSSC incubation periods should be investigated by testing at varied load rates and dwell times.

6. Several tests carried beyond the initiation stage indicate that at some finite depth propagation due to HSSC was not maintained. It is recommended that investigations be conducted to establish parameters affecting HSSC crack depth.

Figure 36. Strain Control Low-Cycle Fatigue Specimen

NOTES:

1. TANGENT POINTS OF 1.750 RAD AND .075 RAD MUST BE BLENDED SMOOTHLY. NO UNDERCUTS OR RIDGES PERMITTED.

2. CENTER OF 1.750 RAD MUST BE LOCATED WITHIN ±.002 OF TRANSVERSE ℄ OF GAGE.

3. ALL DIA TO BE CONC. WITHIN .001 FIR.

4. GA. SECTION TO BE 8 ±3 MICROINCHES AA GRIND FINISH, INCL. INBOARD COLLAR FACES.

5. WORK TO DIM. DO NOT SCALE.

6. IDENTIFICATION MARKINGS PERMITTED ONLY ON ENDS OF SPECIMEN.

7. LOCATE ℄ WITHIN ±.005 OF OVERALL SPECIMEN LENGTH. REFER TO VIEW A FOR ALL OTHER REFERENCES TO THIS ℄.

49

REFERENCES

1. *Stress-Corrosion Cracking of Titanium,* ASTM STP 397 (1966)

2. Gray, H. R., *Relative Susceptibility of Titanium Alloys to Hot-Salt Stress-Corrosion,* NASA TN D-6498 (1971)

3. Ashbrook, R. L., *A Survey of Salt Deposits in Compressors of Flight Gas Turbine Engines,* NASA TN D-4999 (1969).

4. Cotton, J. B., *Stress Corrosion of Titanium Alloys. Stress Corrosion Cracking in Aircraft Structural Materials.* H. G. Cole, ed., AGARD-CP-18 (1967)

5. Gray, H. R., Johnson, J. R., *Effect of Exposure Cycle on Hot-Salt Stress-Corrosion of a Titanium Alloy,* NASA TM X-3145 (1974).

6. Smith, M. P., *MERL Lab Report* No. B-20187, P&WA, Commercial Products Division (1975).

7. Gray, H. R., *Relative Susceptibility of Titanium Alloys to Hot-Salt Stress-Corrosion,* NASA TN D-6498 (1971).

8. Brown, B. F. *Stress-Corrosion Cracking — A Perspective Review of the Problem;* ARPA Order No. 878, NRL Report 7130 (1970).

9. Mahoney, Murry W. and Allen S. Tetelman, *The Effect of Microstructure on the Hot Salt Stress Corrosion Susceptibility of Titanium Alloys,* Metallurgical Transactions — A (October 1976).